Copyright Warning & Restrictions

The copyright law of the United States (Title 17, United States Code) governs the making of photocopies or other reproductions of copyrighted material.

Under certain conditions specified in the law, libraries and archives are authorized to furnish a photocopy or other reproduction. One of these specified conditions is that the photocopy or reproduction is not to be "used for any purpose other than private study, scholarship, or research." If a, user makes a request for, or later uses, a photocopy or reproduction for purposes in excess of "fair use" that user may be liable for copyright infringement,

This institution reserves the right to refuse to accept a copying order if, in its judgment, fulfillment of the order would involve violation of copyright law.

Please Note: The author retains the copyright while the New Jersey Institute of Technology reserves the right to distribute this thesis or dissertation

Printing note: If you do not wish to print this page, then select "Pages from: first page # to: last page #" on the print dialog screen

ABSTRACT

Coating of particles is normally carried out with the use of environmentally unfriendly solvents. Development of dry coating methods is therefore quite important.

A Rotating Fluidized Bed was constructed, instrumented and verified as to operation. Twelve coating experiments were carried out with PMMA 200μm mean diameter as host and alumina 0.25 μm primary particle size as guest with the RFB being operated in the fully fluidized range.

In all analyzed samples, coating was observed. Analysis was carried out on the qualitative basis by SEM and EDX.

EVALUATION OF ROTATING FLUIDIZED BED AS A DRY COATER

by
William Christopher Dunphy

A Thesis
Submitted to the Faculty of
New Jersey Institute of Technology
in Partial Fulfillment of the Requirements for the Degree of
Master of Science in Mechanical Engineering

Department of Mechanical Engineering

January 1999

APPROVAL PAGE

EVALUATION OF ROTATING FLUIDIZED BED AS A DRY COATER

William Christopher Dunphy

Dr. Rajesh N. Dave, Thesis Advisor — Date
Professor of Mechanical Engineering, NJIT

Dr. Robert Pfeffer, Thesis Co-Advisor — Date
Professor of Chemical Engineering, NJIT

Dr. Pushpendra Singh, Committee Member — Date
Professor of Mechanical Engineering, NJIT

BIOGRAPHICAL SKETCH

Author: William Christopher Dunphy

Degree: Master of Science in Mechanical Engineering

Date: January 4, 1999

Undergraduate and Graduate Education:

- Master of Science in Mechanical Engineering,
  New Jersey Institute of Technology Newark, NJ,
  1999

- Bachelor of Science in Mechanical Engineering,
  New Jersey Institute of Technology, Newark, NJ,
  1997

Major: Mechanical Engineering

Minor: Applied Mathematics

Presentations and Publications:

Watano, Pfeffer, Dave and Dunphy, "Dry Particle Coating by a Newly Developed Rotating Fluidized Bed Coater" *Proceedings from AIChE Convention,* Florida, November 1998

This thesis is dedicated to my family; to my Mother, without her help this thesis would have been impossible, to my Father, I wish he were here to read this thesis, and to my siblings, John, Gene, Jim and Dawn, their undying support made this journey easier. Also to my friends who kept me from going insane, especially Tom, Bill and Dr. John Gilchrist, without their infinite patience none of this would exist. Octavius Ad Infinum

ACKNOWLEDGMENT

I would like to express my deepest appreciation to Dr. Rajesh Dave and Dr. Robert Pfeffer, who not only served as my research supervisors, providing valuable and countless resources, insight and intuition, but also for constantly providing support, encouragement and reassurance. Special thanks is given to Dr. Pushpendra Singh for participating in my committee and especially for being a friend. I also wish to thank Dr. Sudhi Mukherjee for going out of his way to help.

TABLE OF CONTENTS

TABLE OF CONTENTS (con't)

CHAPTER 1

INTRODUCTION

1.1 Objective

The objective of this thesis is to evaluate the Rotating Fluidized Bed (RFB) as a dry coating (RFBC) machine. It is believed that the magnification of the impact forces by RFB technology will create enough shear and normal forces to coat a guest onto a host. The shear force, to deagglomerate and smear the guest onto the host, and the normal force to impregnate the guest into the hosts surface.

There are two main components to this thesis. First a laboratory scale rotating fluidized bed has been designed, constructed and instrumented for data acquisition. In the second part of this thesis, the performance of the RFB is verified and evaluated as a dry coating machine using 200μm PMMA as host and 5% 0.25μm primary alumina as guest.

1.2 Motivation

Most current methods of coating are carried out in a wet form. Colloidal systems and spray type systems as well as others usually employ a volatile and toxic solvent that must be evaporated off into the atmosphere and/or stored as toxic waste. For example, a Wurster type coater [8] is a standard type fluidized bed with a center tube where the coating guest is in a suspension that is sprayed into the system,

leaving the solvent to be evaporated off into the atmosphere or to be captured by expensive equipment.

Dry coating uses no solvent and produces no residue that must be stored. This should be viewed as an important development in light of current environmental regulations both self imposed and government imposed.

1.3 Background Information

Fluidization is the operation by which fine solids are transformed into a fluid like state through contact with a gas or liquid [4]. This was first proven by Fraser and Yancey in 1928 [4]. A fluidized bed has the following positive characteristics;

- Superior mixing
- High rate of heat transfer
- Temperature uniformity
- Accelerated reaction due to available surface area
- Lower pressure drop than fixed bed

The RFB has all the desirable characteristics of a standard fluidized bed plus the ability to replace the gravity term in the standard bed equation by a centrifugal term (see Appendix C) which can be adjusted by increasing or decreasing the rate of rotation of the distributor.

Consider a standard fluidized bed (see Fig 1.3). It consists of a tube with a distributor (porous ceramic, sintered metal, wire cloth etc...) fixed near the bottom. Fluidization gas is introduced at the bottom at superficial velocity *Uo* and passes through the distributor and then through the particle bed which rests on the

distributor. At zero velocity and until minimum fluidization velocity, Umf, the bed is said to be packed. At this point, Umf, the bed enters the fully fluidized regime. This regime is marked by a characteristic plateau where the whole bed is fluidized. At the time of fluidization, bubbling starts, but is negligible until some Umb when bubbling becomes vigorous(see chapter 3). After the bubbling reaches a certain point, entrainment (elutration) begins and material is ejected.

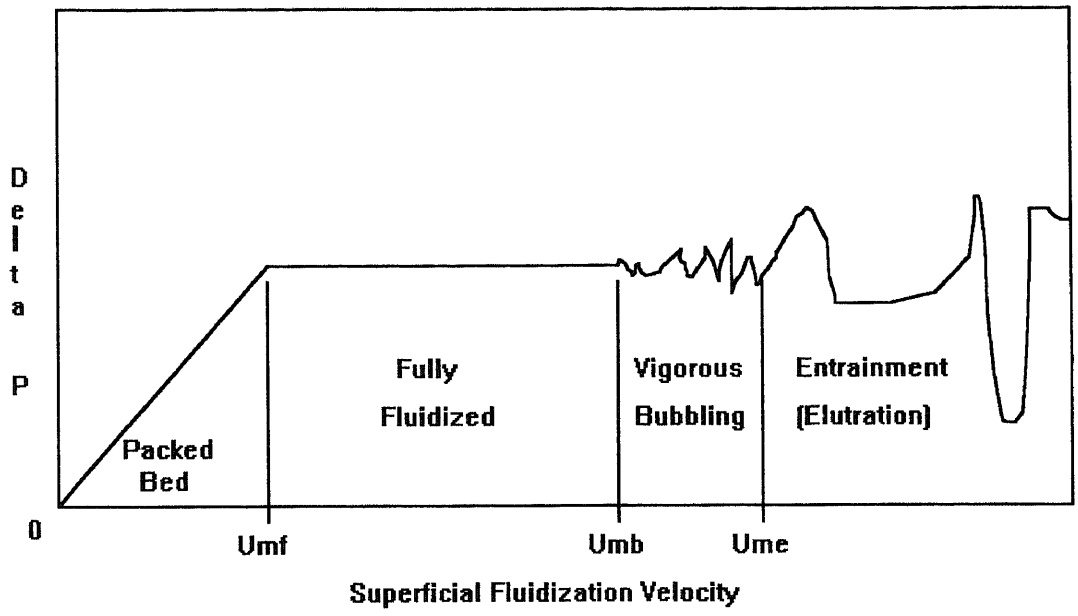

Fig. 1.1 standard bed fluidization graph

In a RFB the centrifugal force increases with depth in the bed. The bed remains packed until a minimum velocity Umf, when the inner surface of the bed fluidizes. When the superficial velocity reaches a critical velocity Umfc, the whole bed is fluidized. It is also at this point that bubbling begins, but it is negligible up to Umb.(see Fig 1.2) When the velocity reaches Ume, elutration begins.

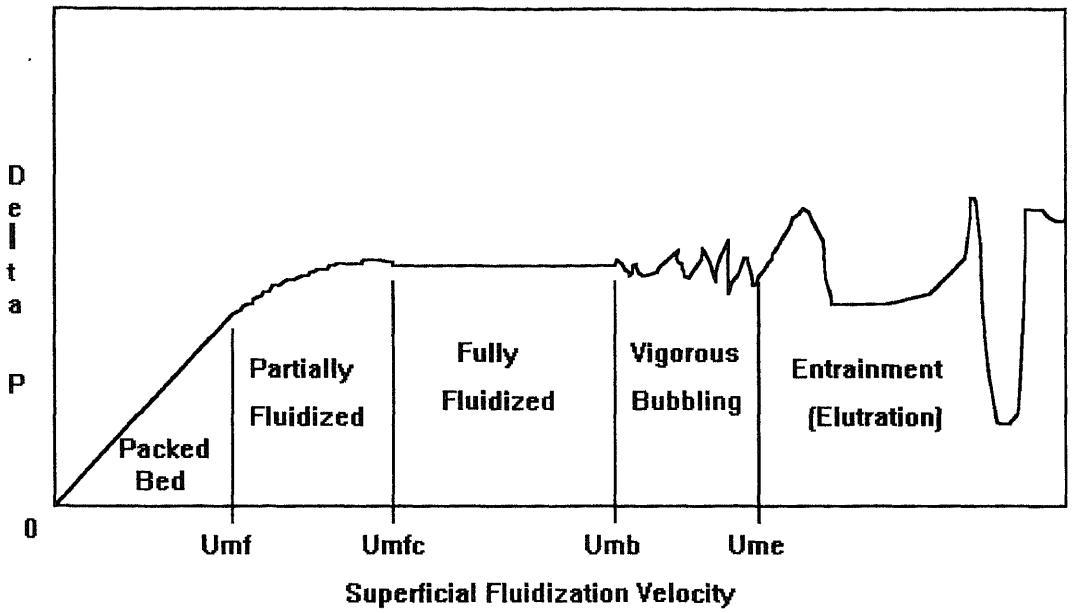

Fig. 1.2 RFB fluidization graph

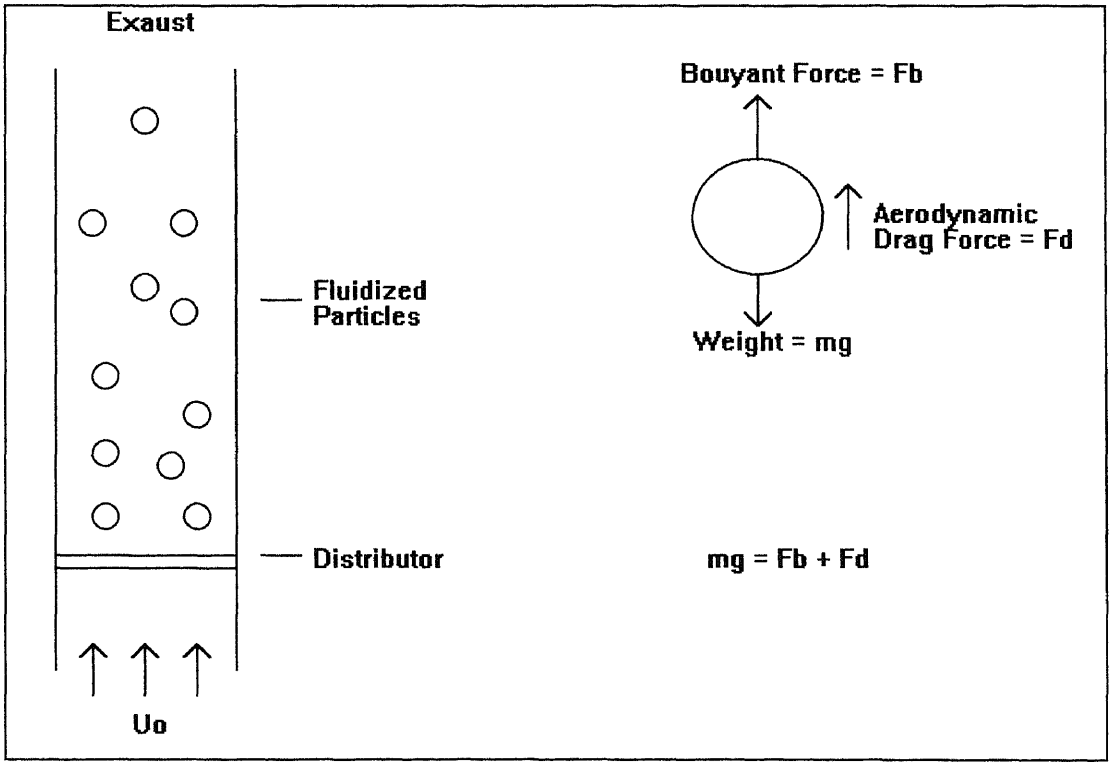

Fig. 1.3 Standard fluidized bed with free body diagram and force balance

The force balance can be written as:

$$mg = F_b + F_d$$

$$mg = \rho_g g V + F_d$$

$$mg - \rho_g g V = F_d$$

$$\left(m - \rho_g V\right) g = F_d$$

As can be seen by the force balance, the only thing that can be done to increase the flow rate of fluidization gas, and therefore the aerodynamic drag, is to increase the effective accelleration of gravity.

This can be achieved by rolling the distributor into a cylinder and rotating it as in the RFB (see Fig 1.4). The force balance for the RFB can be written as:

$$m\omega^2 r = F_b + F_d$$

$$m\omega^2 r = \rho_g \omega^2 r V + F_d$$

$$m\omega^2 r - \rho_g \omega^2 r V = F_d$$

$$\left(m - \rho_g V\right) \omega^2 r = F_d$$

By increasing the angular velocity of the bed the aerodynamic drag force must be increased to achieve fluidization, this inturn magnifies the impact forces. This feat can be achieved by placing endcaps on the cylindrical distributor, one with an exhaust outlet, and placing the assembly in a pressurized plenum. Thus the flow is directed through the bed.

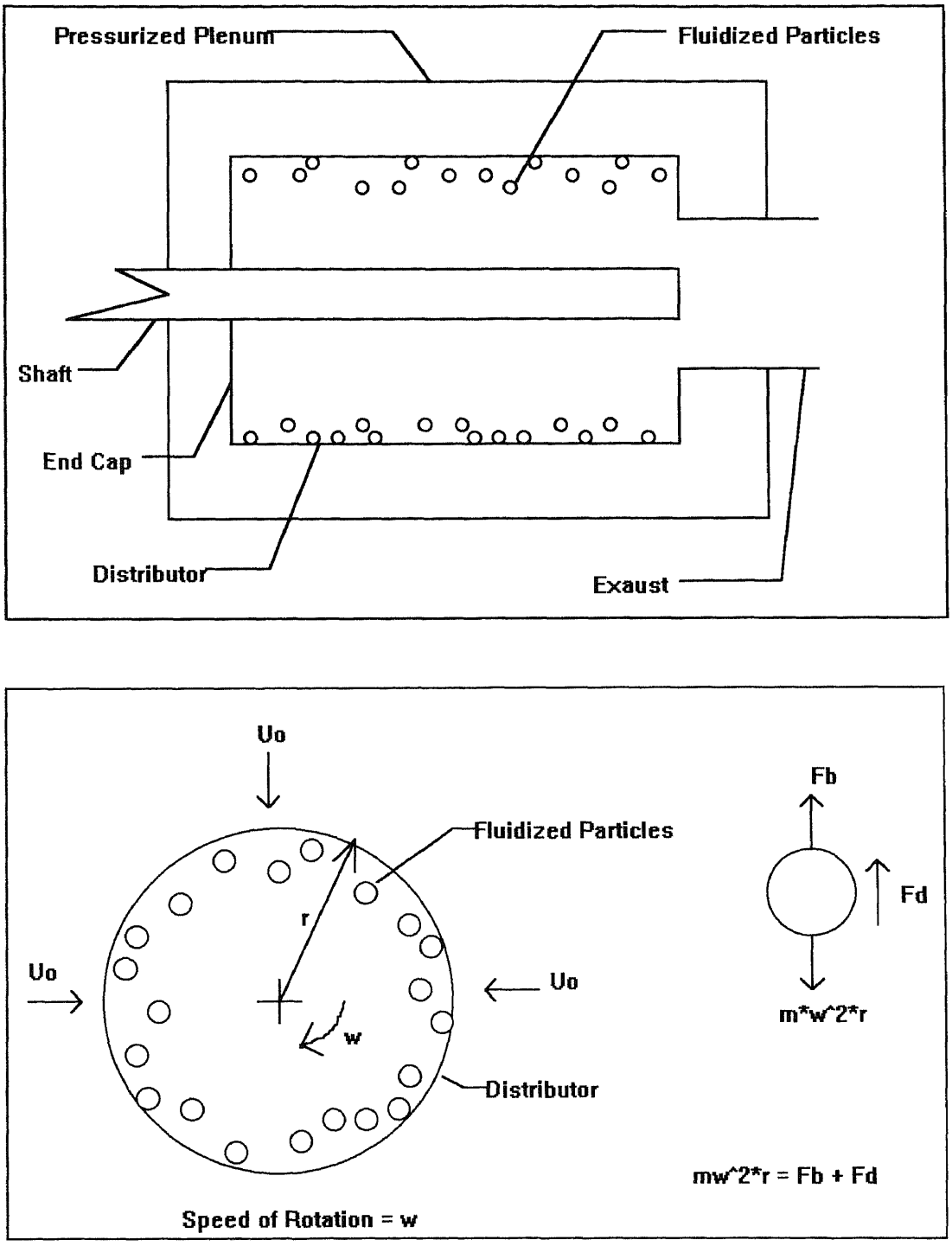

Fig 1.3 Rotating fluidized bed side view (top) and front view (bottom) with free body diagram and force balance

As can be seen in the force balance, the higher the rotation rate, the more gas can be passed through the bed.

This increase in gas flow coupled with the increased effective weight will induce vigorous mixing accompanied by increased impact forces, most importantly shear. It is this shear which will do most of the coating of the host onto the guest.

CHAPTER 2

DESIGN AND BUILDING OF RFB

2.1 Statement of Problem

In order that the machine be a rotating fluidized bed the following criteria must be met;

- The distributor must be cylindrical
- The distributor must be rotated during operation
- The distributor must rotate inside a pressurized plenum during operation
- The inside of the distributor must be exhausted to the outside of the plenum

2.2 Choice of Materials

As sample size is to be kept small, about 30 grams, a readily available thin wall steel cylinder of 2.25 inch inner diameter and 3 inch length was chosen to be used as a distributor. The plenum must be of appropriate size as to contain the distributor, a readily available 4 inch PVC schedule 40 pipe was selected. During prototyping it was decided that the bed should be visible from the outside during operation so readily available acrylic sheeting was selected for distributor end plates and plenum housing end plates as well as the hatch in the front plenum end plate. In order that the plenum be sealed around the rotating exhaust nozzle, a

special seal made of moly impregnated fiberglass was constructed by National Ready Seal. The shaft was made of readily available 1/2 inch drill rod. Teflon® bushings were procured for rear plenum plate penetration point and exhaust nozzle. It was later discovered that the seal and nozzle were of incompatible material so a stainless steel Ready Sleeve® was fitted to the exhaust nozzle. The PVC plenum chamber was gasketed to the acrylic end plates using red rubber plumbers gasket. The bearings were easily procured mounted in pillow blocks from a machinist's supply. The motor was a Dayton DC model with RPM controller. All parts were mounted to a 2 X 12 inch yellow pine plank.

2.3 Engineering Analysis of Particle Forces

G forces imparted on particle at wall of distributor;

$$F = ma = mr\omega^2 \quad (1)$$

$$a = r\omega^2 = \frac{57.15 * 10^{-3} m}{2} * (RPM * \frac{\pi}{30})^2 * \frac{1}{9.81 \frac{m}{s^2}} \quad (2)$$

RPM	a [g]
300	**3**
600	**11.5**
900	**26**
1200	**46**
1500	**72**

2.4 Choosing Convenient Dimensions

In order that the RFB be built with a minimum of special tools, all components purchased were selected with respect to each other and with respect to available cutting tools. The motor had a 5/8 inch output shaft and the drive shaft selected for the RFB was 1/2 inch. A rubber coupler was commercially available to join the two. The drive shaft bearings were pillow block units and were available in the required 1/2 inch inner diameter size. A Teflon® bushing of 1/2 inch ID and 3/4 inch OD was selected to bush the drive shaft through the rear plenum plate, another bushing selected from the same series of 1 inch ID and 1 1/4 inch OD served as the exhaust nozzle. These selections were viewed as excellent as the rear bushing would not have to be lubricated so as to ward off contamination of the sample. The same view was taken with the bushing that was to serve as exhaust nozzle, but, a poor choice of seal material by National Ready Seal engineers required that a Ready Sleeve® made of stainless steel be installed over the nozzle. Another parameter was also satisfied by virtue of convenient dimensions on the OD of the bushings as they were of readily available drill sizes.

2.5 Manufacture of RFB

The only special tools used in the manufacture of the RFB prototype were a Craftsman® router table and router, and a small drill press. Fixtures were made with a flat board and wooden dowels to make the perfectly circular end caps for

the distributor, and to make the circular recesses in the end plates for the plenum.. The correct size center holes were drilled into the acrylic plastic and were passed by the router bit by hand.

In order that the distributor be slotted properly, a 1/4 inch four flute end mill was fitted to the router table. A fixture made of red oak was slotted and eased on the top edge and the pre drilled steel distributor cylinder was screwed down firmly and the whole fixture was passed over the end mill by hand..

The use of threaded rod was maximized so as to reduce the cost of manufacture. All components are held together and mounted using threaded rod.

CHAPTER 3

VERIFICATION OF RFB

3.1 Generation of Fluidization Curve

In order that the RFB built in this thesis actually performs as a rotating fluidized bed, and, to insure that the coating attempt be made in the fluidized region, fluidization curves must be generated for this machine.

The first step in generating the fluidization curves is to take differential manometer readings at incremental steps of air flow with the distributor empty. After this is performed at all desired rotation speeds, the distributor is loaded with a 30 gram sample of the 200μm PMMA host. The RFB is then run and manometer readings taken at the same air flow increments as previous. The data is then subtracted, the data points generated with the empty distributor are subtracted from the points taken with the sample in the distributor. These points are then graphed on the ordinate while the equivalent superficial velocity with respect to air flow are graphed on the abscissa (see Fig 1.1).

If one consults the fluidization graph, one can see the reasonably linear packed bed region clearly. Next is the partially fluidized regime. This is followed in most cases by a fully fluidized plateau. This is most evident in the 600 RPM graph and is absent in the 1500 RPM graph. During the fully fluidized plateau regime, the bubbling regime takes place. The bubbling is negligible in the beginning and gradually increases until elutriation (entrainment or ejection). This type of

behavior is typical of Geldart type A particles [9]. It should be noted that in a Rotating Fluidized Bed, heavy bubbling can lead to entrainment as when a bubble bursts the particles are flung up into the distributor and are disconnected from their effective acceleration leaving them too light to remain in the system.

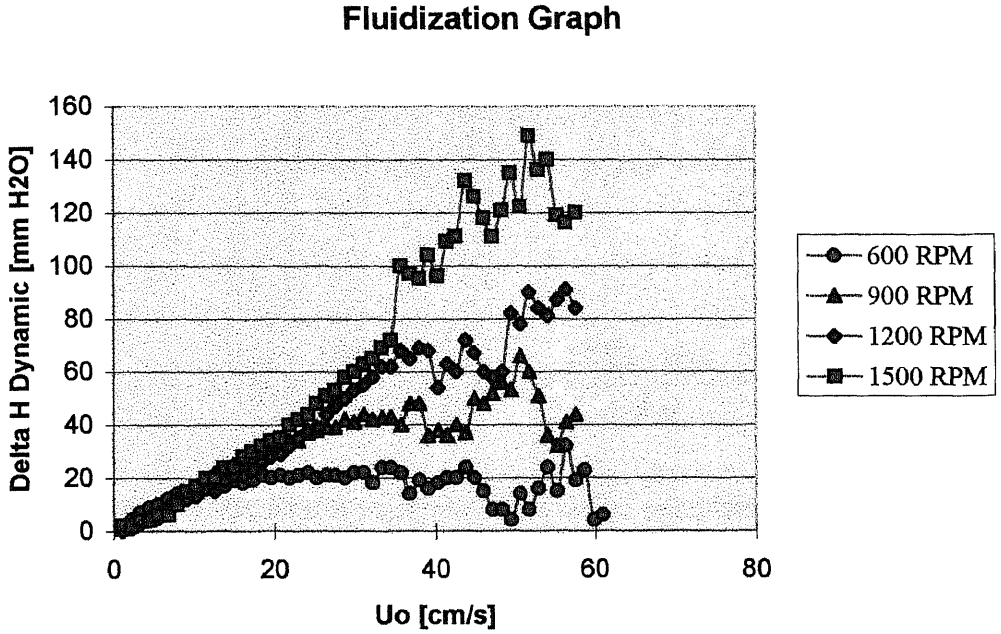

Fig. 3.1 Experimental calibration data

It can be seen that for 600 RPM full fluidization occurs at approximately 12 cm/s and ends at approximately 36 cm/s followed by the bubbling regime. For 900 RPM full fluidization starts at approximately 25 cm/s and ends at approximately 36 cm/s followed by its bubbling regime. For 1200 RPM full fluidization begins at approximately 35 cm/s and ends at approximately 40 cm/s followed by its bubbling regime. 1500 RPM exhibits no plateau, this RFB is incapable of safely handling the pressure difference and therefore the superficial velocity to fluidize this material at this RPM.

3.2 Comparison of Experimental Data to Theory

The accepted model of Rotating Fluidization is derived from the Ergun equation, the following derivation is taken from [1]. Pressure drop as a function of superficial gas velocity is based on the semiempirical equations of Chen [8] modified by Kao [1]. In the packed bed region, the pressure drop is given by;

$$\frac{dP}{dr} = \phi_1\left(\frac{U_o r_o}{r}\right) + \phi_2\left(\frac{U_o r_o}{r}\right)^2 + \rho_f r\omega^2 + \frac{\rho_f U_o^2 r_o^2}{\varepsilon^2 r^3}$$

Where;

$$\phi_1 = \frac{150(1-\varepsilon)^2\mu}{\varepsilon^3(\phi_s d_g)^2}; \phi_2 = \frac{1.75(1-\varepsilon)\rho_f}{\varepsilon^3\phi_s d_g}$$

Which is based on the Ergun equation. The major contribution is from the drag force per unit volume, that is the first two terms. The remaining two terms add up to less that one percent and may be neglected. Now we are left with;

$$\frac{dP}{dr} = \phi_1\left(\frac{U_o r_o}{r}\right) + \phi_2\left(\frac{U_o r_o}{r}\right)^2$$

Which is integrated thus;

$$\int_{P_i}^{P_o} dP = \phi_1 U_o r_o \int_{r_i}^{r_o} \frac{dr}{r} + \phi_2 U_o^2 r_o^2 \int_{r_i}^{r_o} \frac{dr}{r^2}$$

Which results in;

$$\Delta P = \phi_1 U_o r_o \ln\left(\frac{r_o}{r_i}\right) + \phi_2 U_o^2 r_o^2\left(\frac{1}{r_i} - \frac{1}{r_o}\right)$$

For the fully fluidized plateau the original equation takes the form of;

$$\frac{dP}{dr} = (\rho_g - \rho_f)(1-\varepsilon)r\omega^2 + \rho_f \varepsilon r\omega^2 + \frac{\rho_f U_o^2 r_o^2}{\varepsilon r^3} + \frac{\rho_f U_o^2 r_o^2}{\varepsilon^2 r^2}\frac{d\varepsilon}{dr}$$

And as in the packed bed region, the three right terms are negligible resulting in;

$$\frac{dP}{dr} = (\rho_g - \rho_f)(1-\varepsilon)r\omega^2$$

Integrating;

$$\int_{P_1}^{P_2} dP = (\rho_g - \rho_f)(1-\varepsilon)\omega^2 \int_{r_i}^{r_o} r dr$$

Which results in;

$$\Delta P = (1-\varepsilon)(\rho_g - \rho_f)\omega^2 (r_o^2 - r_i^2)/2$$

3.3 Graphical Comparison

The above equations are graphed along with the experimental data in order that a comparison be made. A void fraction of 4.2 was found to be a good approximation, verifying Wen and Yu's correlation [11]. To make up the difference between actual and ideal situations a fully fluidized correction factor of 0.78 provided good agreement of the data with the theory. In the following graphs, series 1 is the experimental data, series 2 is the fully fluidized theory and series 3 is the packed bed theory. Because of the unwieldy nature of the partially fluidized theory equation it is omitted in these graphs (see appendix C).

The three rotometers used to regulate the mass flow of air into the system behaved in different ways. Meter one and two regulated up to 600 SCFH and were steady and easy to use. However, meter three that regulated from 600 SCFH

and above had wild fluctuatuions and may have contributed to the bubbling and elutration from that point on. If Q = 600 SCFH then Uo = 34.5622 cm/s.

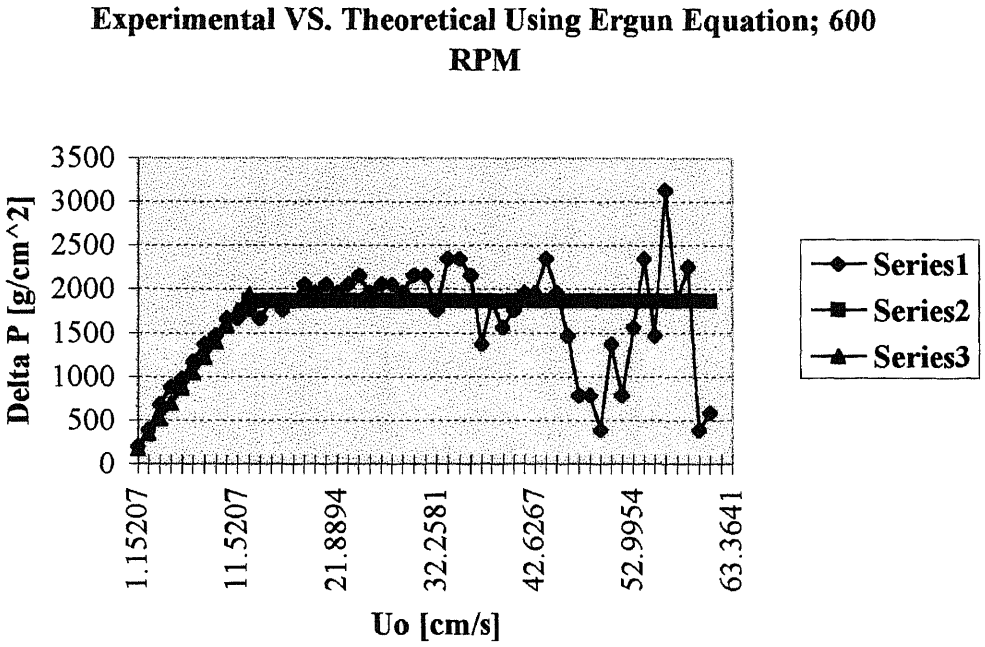

Fig 3.2 Comparison of theory to data 600 RPM

Good agreement of packed bed equation accompanied by an underestimation of the fully fluidized plateau. Heavy bubbling is evident before the ejection region.

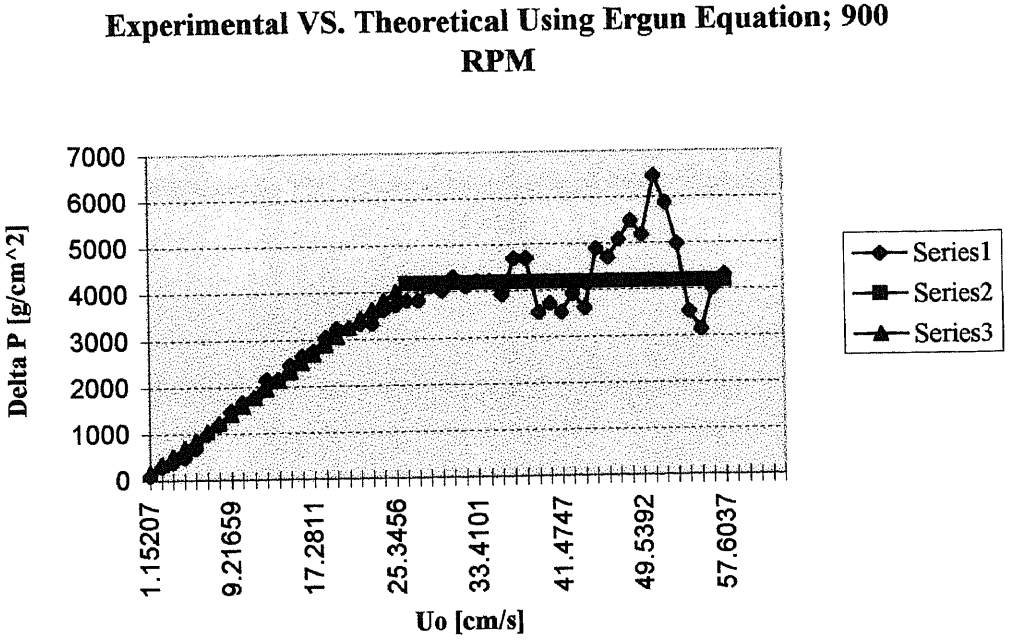

Fig. 3.3 Comparison of theory to data 900 RPM

Excellent agreement in both packed bed and fully fluidized plateau.

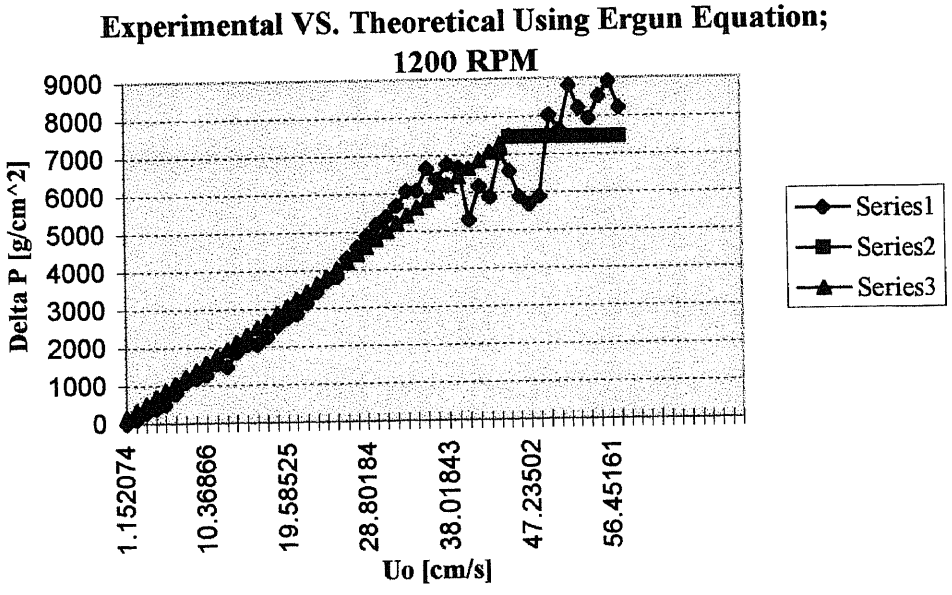

Fig. 3.4 Comparison of theory to data 1200 RPM

Good agreement in packed bed region accompanied by an ambiguous fully fluidized region.

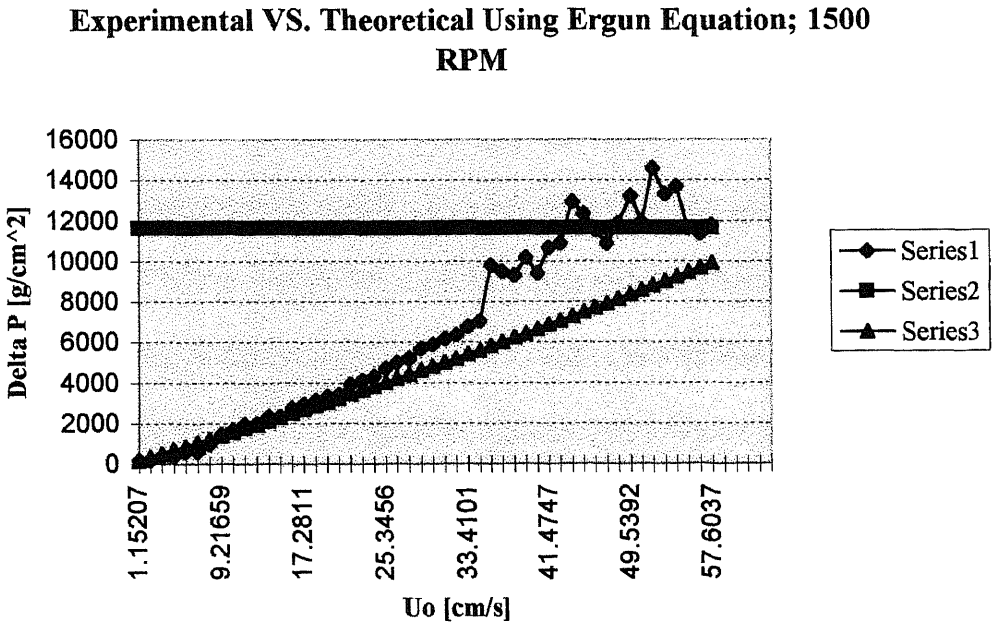

Fig. 3.5 Comparison of theory to data 1500 RPM

Good agreement during initial packed bed region accompanied by divergence, no fully fluidized plateau realized.

CHAPTER 4

COATING EXPERIMENTS

4.1 Choice of Rotation Speed

Out of four speeds tested in chapter 3, two were selected for coating attempts, 900 RPM and 1200 RPM. 600 RPM exhibits a long and flat plateau where operation of the RFB in the fluidized region would be easily accomplished, but, the fact that only 3g's are generated by the rotation dictates that a higher RPM is needed for coating to occur. 1500 RPM was discarded as there was no fluidization present.

4.2 Choice of Fluidization Velocity

Experiments were run at a multiple of minimum fluidization velocity. For 900 RPM the values ranged from 600 SCFH to 720 SCFH. For 1200 RPM the values ranged from 780 SCFH to 1000 SCFH. If one checks the fluidization graph from chapter 3, some of these values are within the bubbling and/or ejection region for PMMA alone. The reason for this is that the presence of alumina seems to change the system sufficiently to prevent ejection, and, after performing the experiment in the fluidization region it was decided to raise the flow rate to maximize the interparticle forces. Future researchers of this topic should note that perhaps calibration of the RFB with the binary system would be more appropriate. This increase is acceptable as after processing almost all of the sample remained in the bed. This decision was made after observing the angle of repose of the sample

after processing. It was felt that the first three runs could have had a larger increase in AOR had a higher gas flow rate been used. The latter experiments exhibited an increased AOR as compared to the first three. These AOR measurements were made by eye in the sample jar.

4.3 Experimental Grid

The 12 experiments were carried out as follows:

Exp. #	Δp [mm H2O]	RPM	Run Time [min.]	Uo [cm/s]	Q [SCFH]
1	72	900	10	34.5622	600
2	72	900	20	34.5622	600
3	72	900	30	34.5622	600
4	110	900	10	41.4747	720
5	128	900	20	37.4424	650
6	128	900	30	37.4424	650
7	156	1200	10	44.9309	780
8	156	1200	20	44.9309	780
9	156	1200	30	44.9309	780
10	236	1200	10	57.6037	1000
11	236	1200	20	57.6037	1000
12	248	1200	30	57.6037	1000

4.4 Results

Although only a qualitative analysis was possible results were considered good. The RFB was verified and coating of alumina on PMMA was achieved. Looking at the raw SEM images in Appendix B, coating or an ordered mixture has clearly taken place on all samples tested. Due to limited time for SEM analysis, only seven of the twelve raw runs were analyzed.

In order that the coating condition be verified, three samples were sonicated for one minute in tap water and then subjected to further SEM analysis followed by EDX elemental mapping for aluminum.

Comparing sample #12 before and after sonication (see fig 4.1), the image on the right appears to retain coating despite sonication of the raw sample on the left. This shows that this is not just an ordered mixture but actual dry coating has taken place.

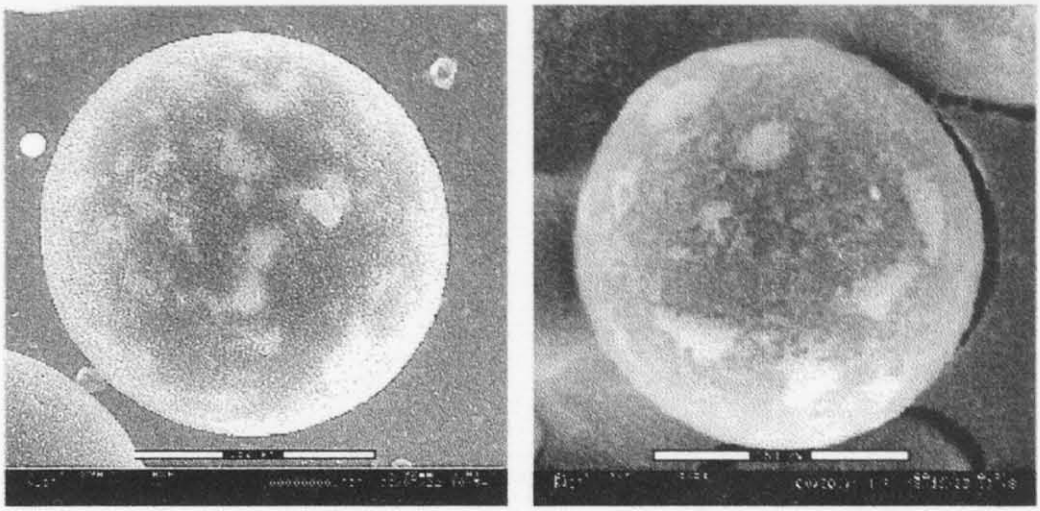

Raw **Sonicated**

Fig 4.1 SEM images of batch #12 before and after sonication of 1 min.

Although still a qualitative test, an EDX elemental mapping was carried out on all three batches that were sonicated. In all three cases, coating was observed. Shown in Fig 4.2 is sample #10 run for 10 min. (see chapter 4.3) and exhibits a reasonable amount of discreet coating. Sample #12 in fig 4.4 is run at the same settings (RPM and Q) for 30 min. and shows a heavier coating. This suggests that coating increases with time (see fig. 4.5). Sample #11 (fig. 4.3) shows an unfamiliar heavy and flaky unsymmetric coating and is considered anomalous and is being disregarded in these results.

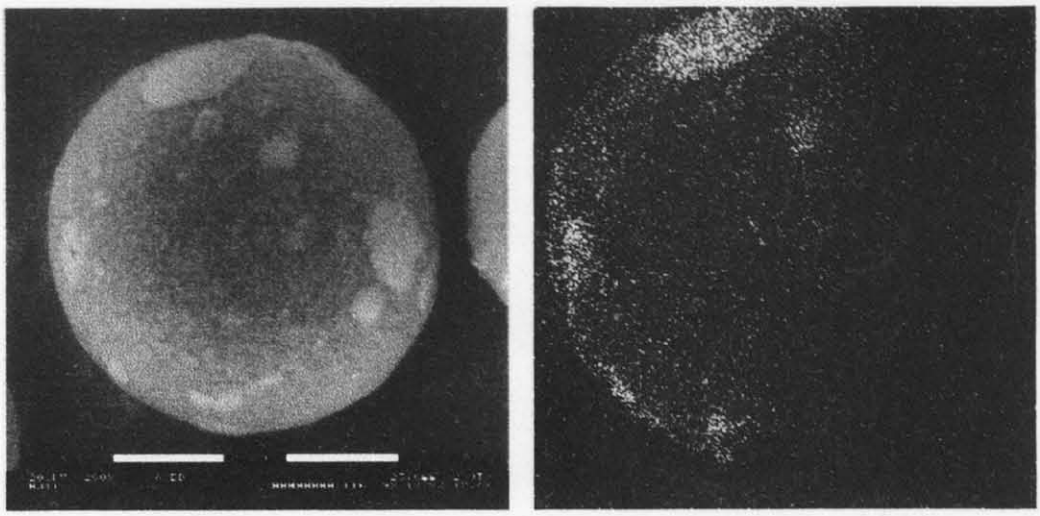

Fig 4.2 Sample #10 sonicated for 1 min. SEM/EDX for Al

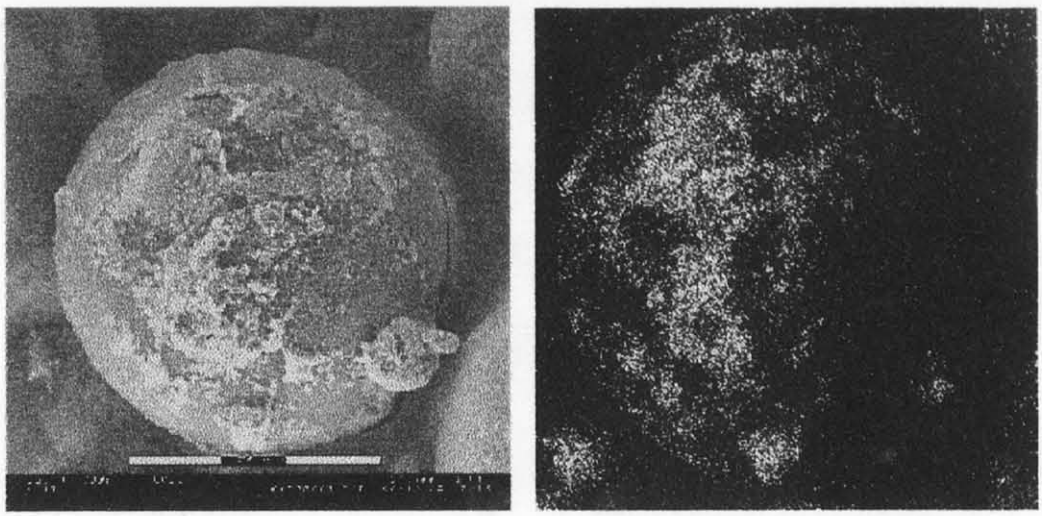

Fig 4.3 Sample #11 sonicated for 1 min. SEM/EDX for Al

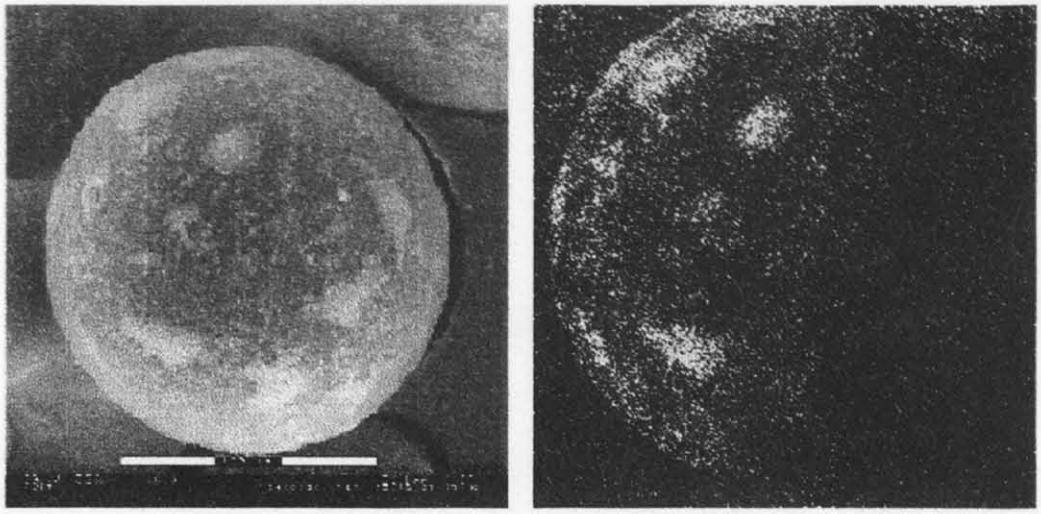

Fig 4.4 Sample #12 sonicated for 1 min. SEM/EDX for Al

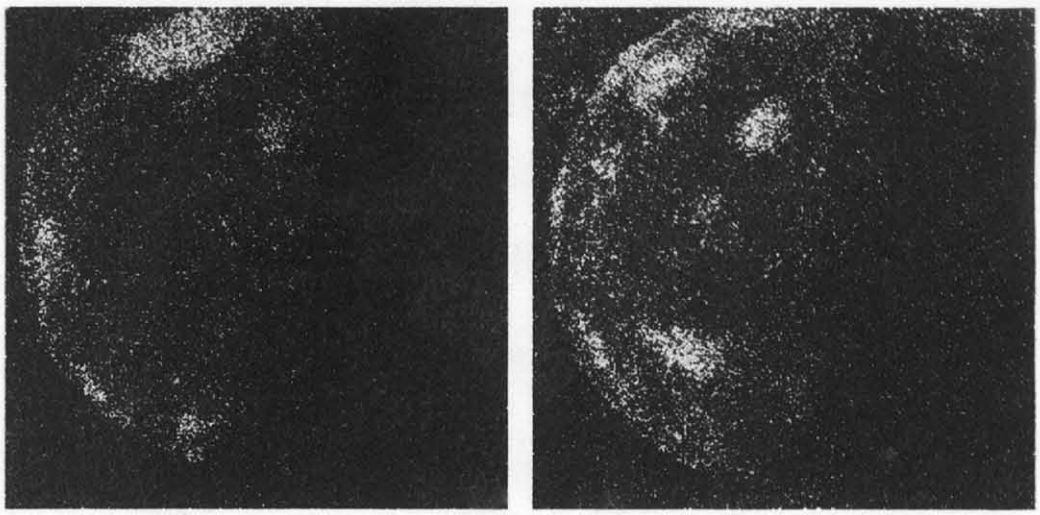

Fig 4.5 Comparison of EDX results of sample 10 and sample 12

4.5 Conclusions and Recommendations

This thesis has established the RFB as a feasible method to carry out dry coating. Coating condition requires further analysis as does thickness of coating with respect to time. Scale up of this RFB technology needs to be investigated as well

as a continuous process instead of a batch system. Most important of all would be to identify and describe the mechanism of coating in the RFB.

APPENDIX A

DETAIL DRAWINGS

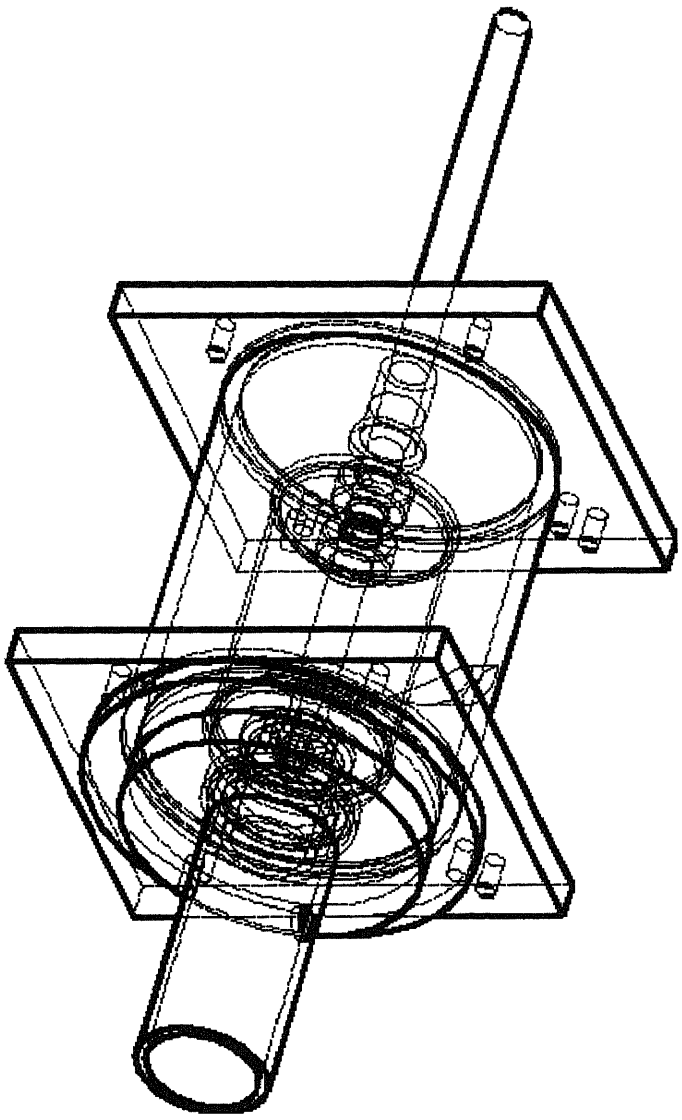

Fig A.1 RFB assembly (hidden line)

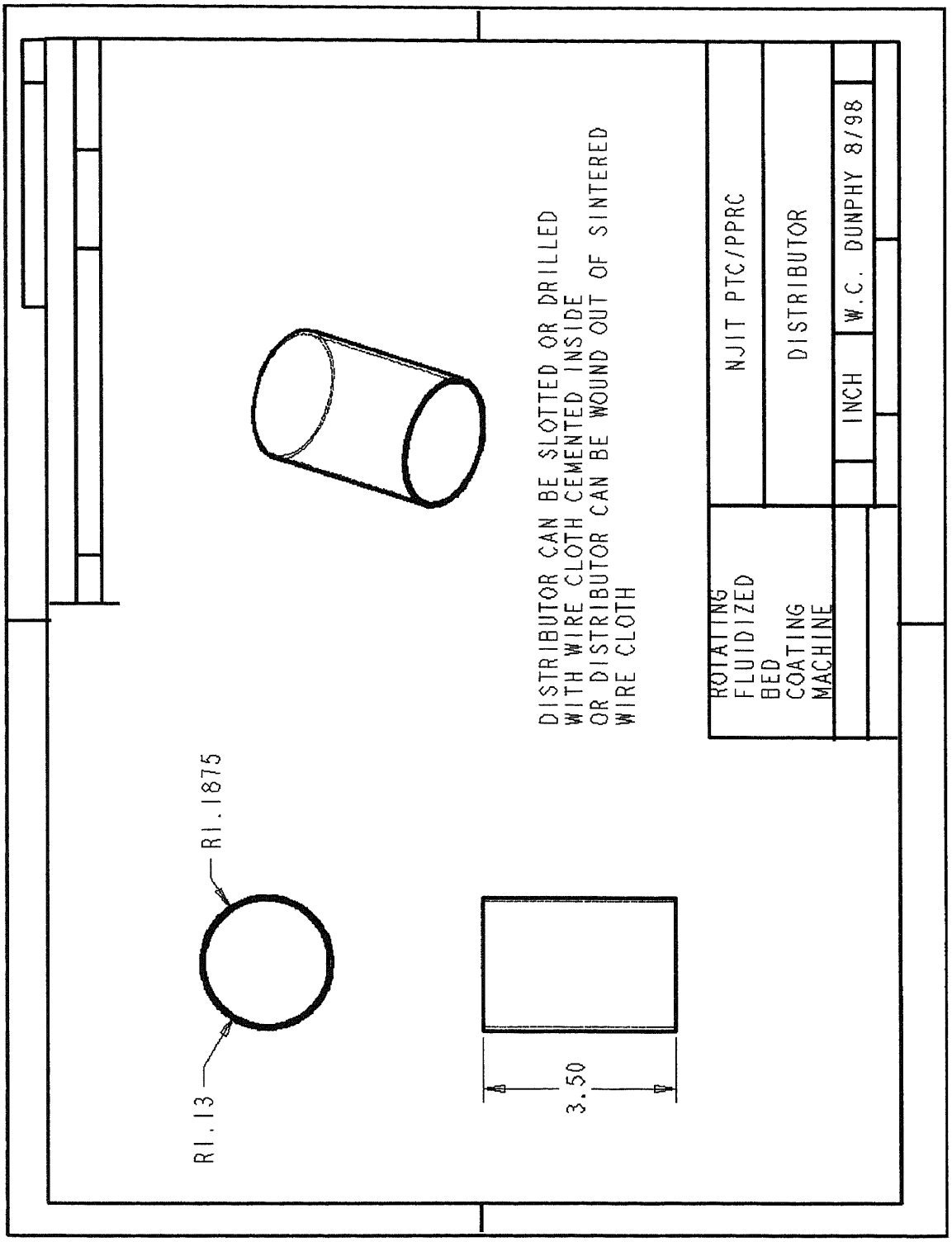

Fig A.2 distributor

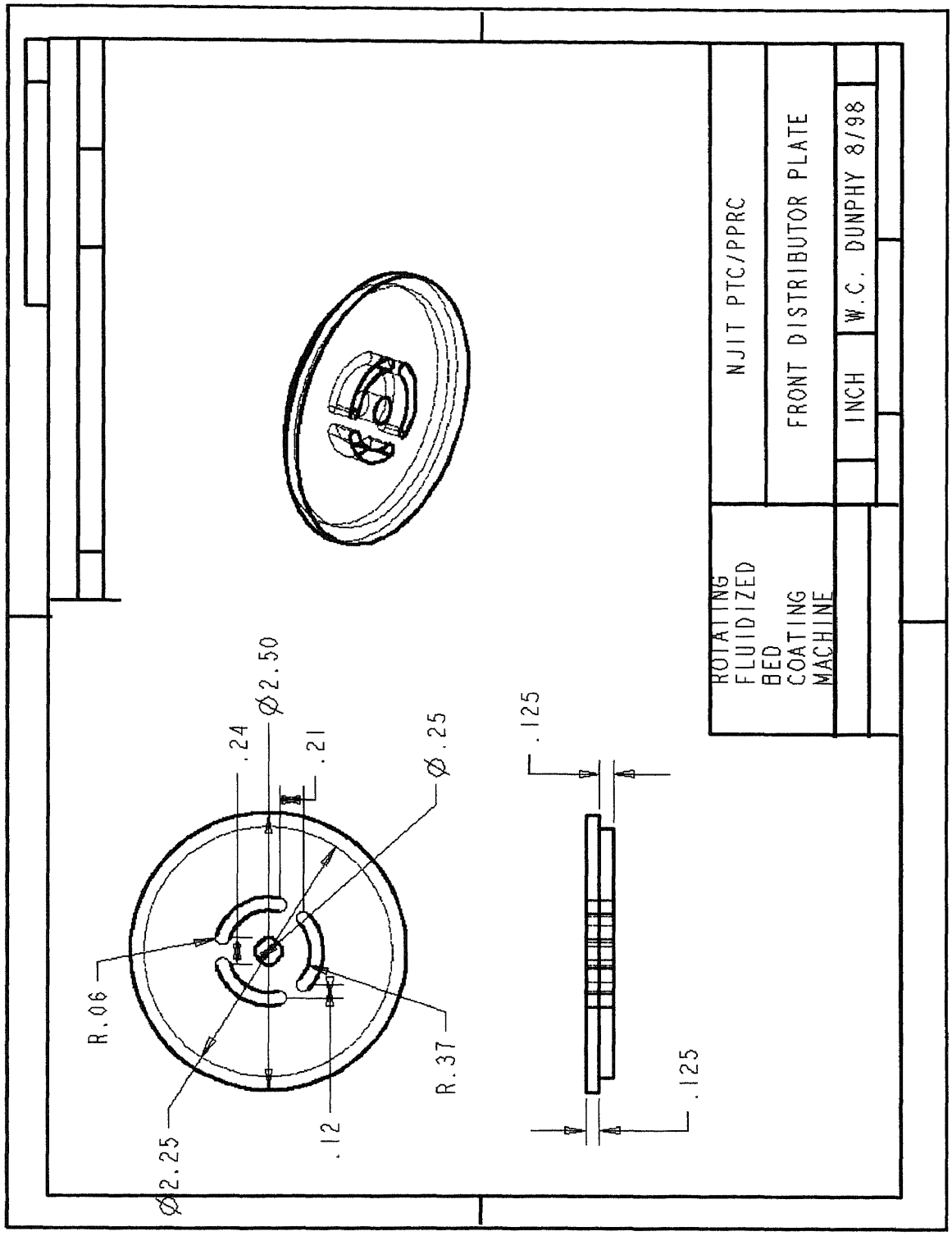

Fig A.3 front distributor plate

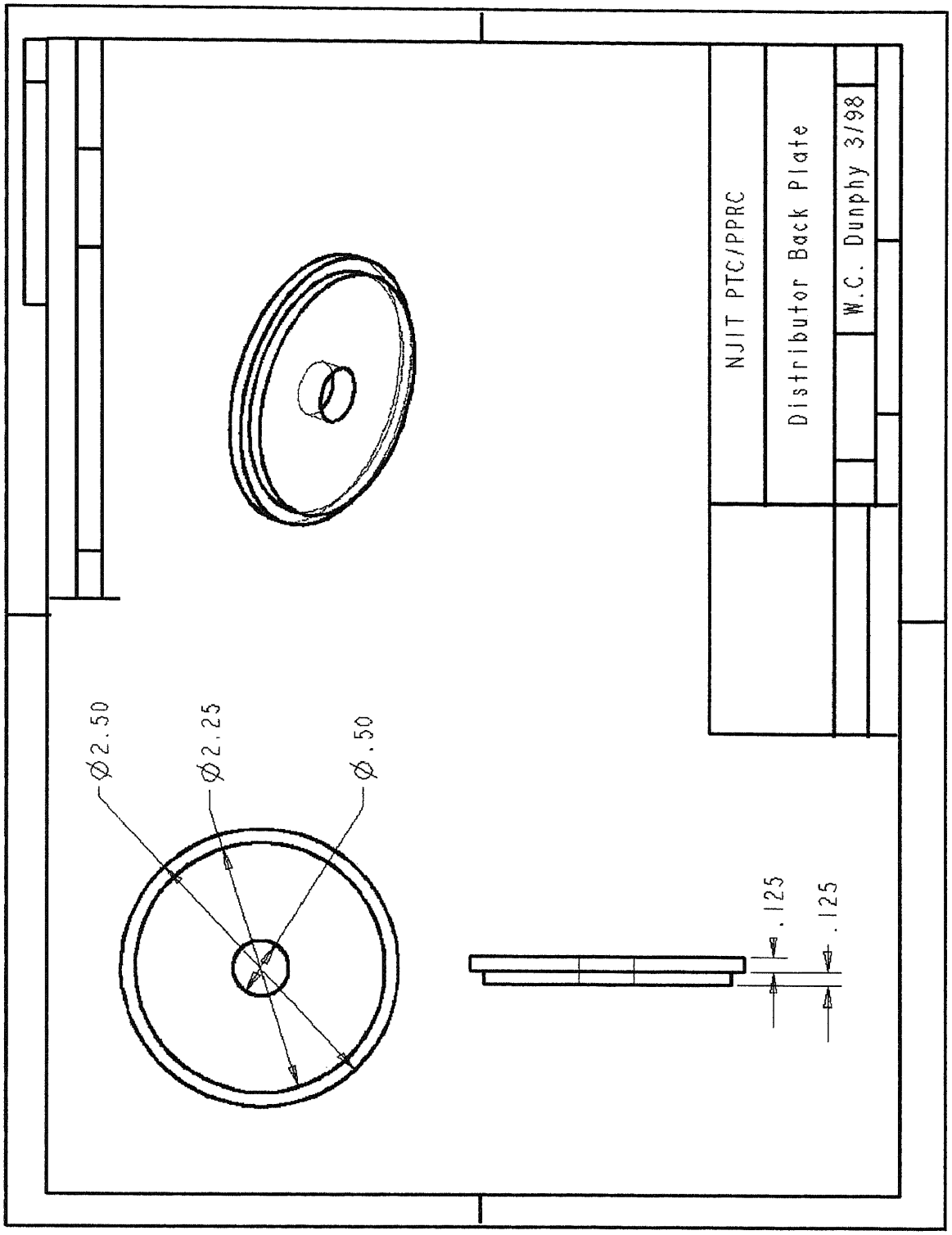

Fig A.4 back distributor plate

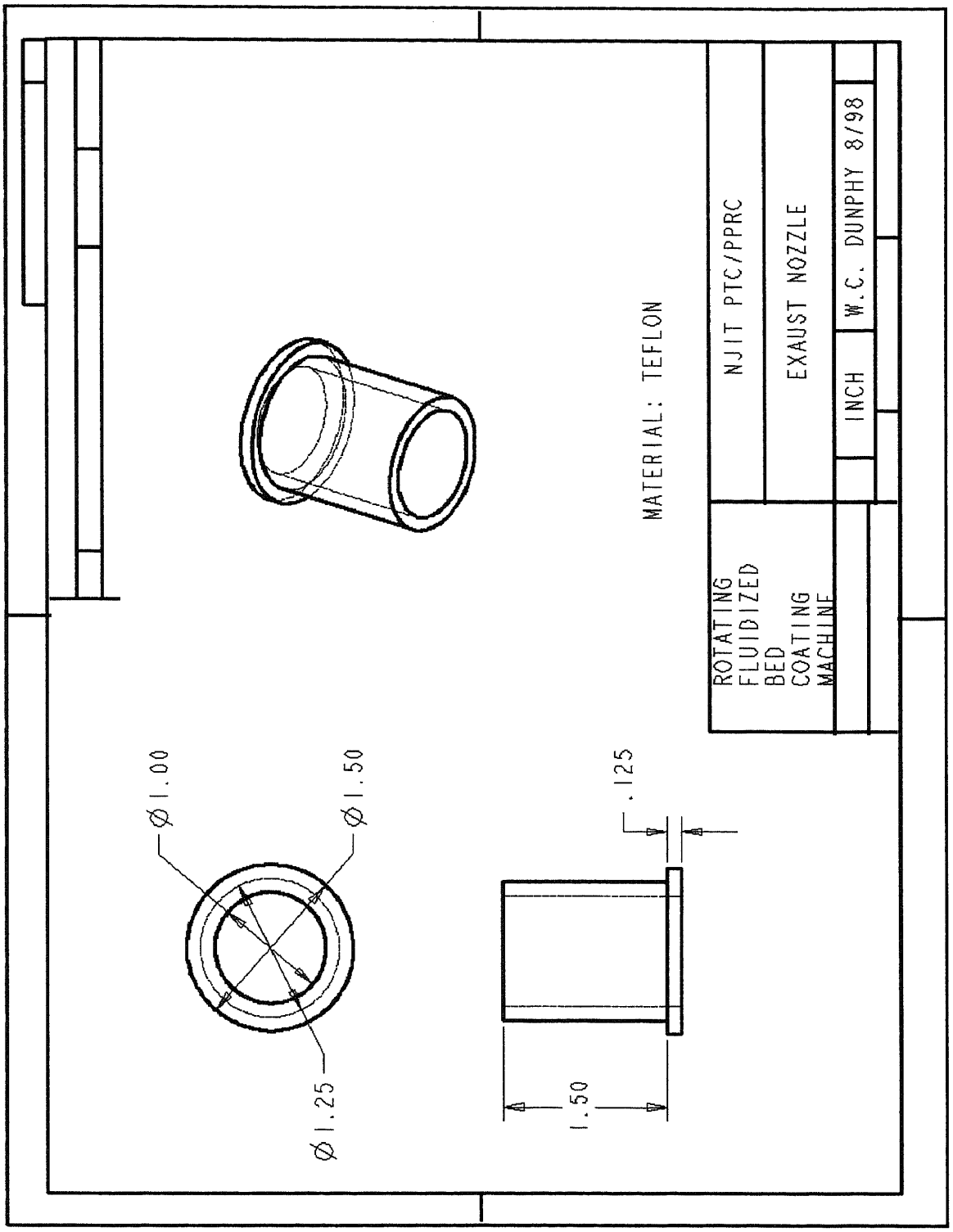

Fig A-5 exaust nozzle

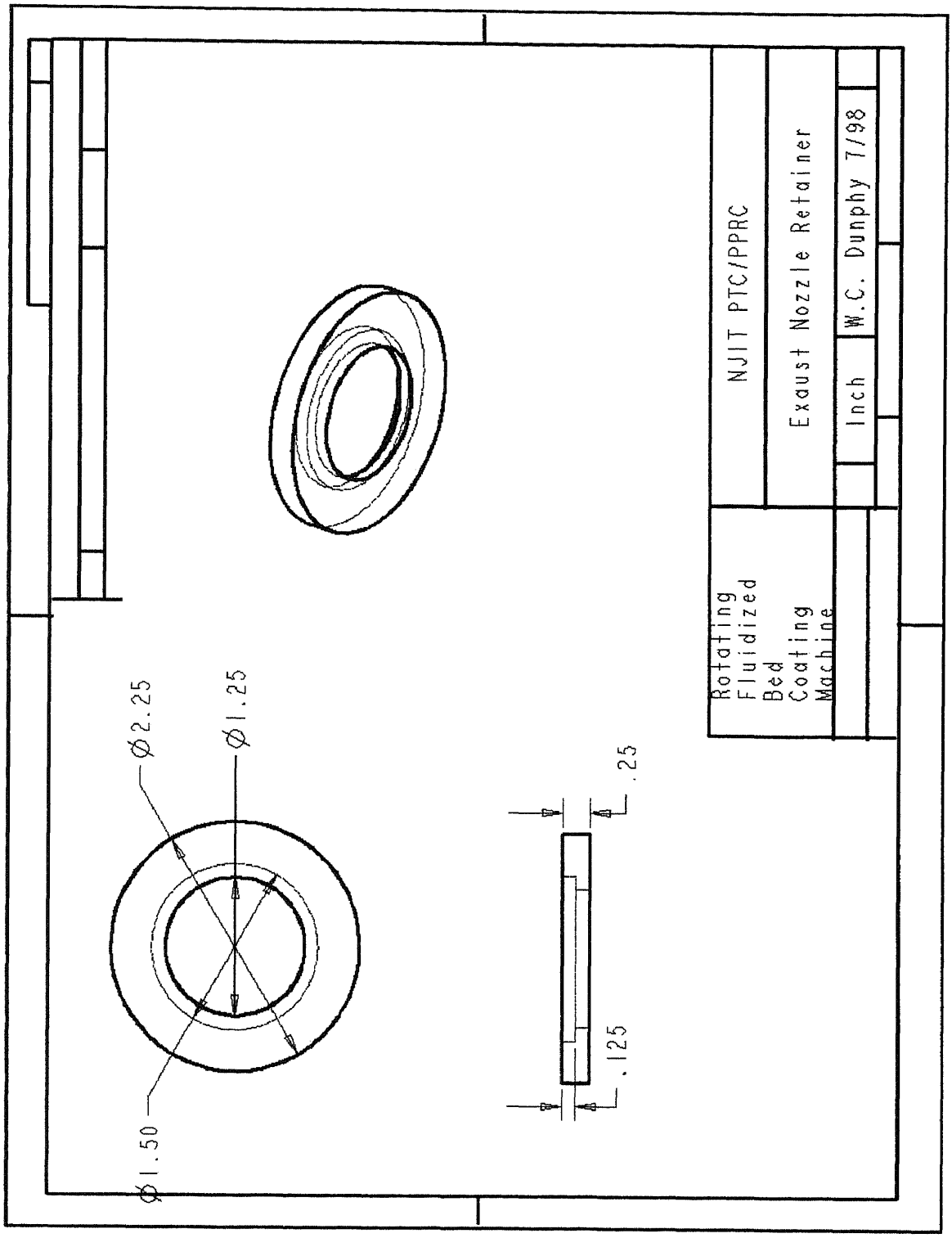

Fig A.6 exaust nozzle retainer

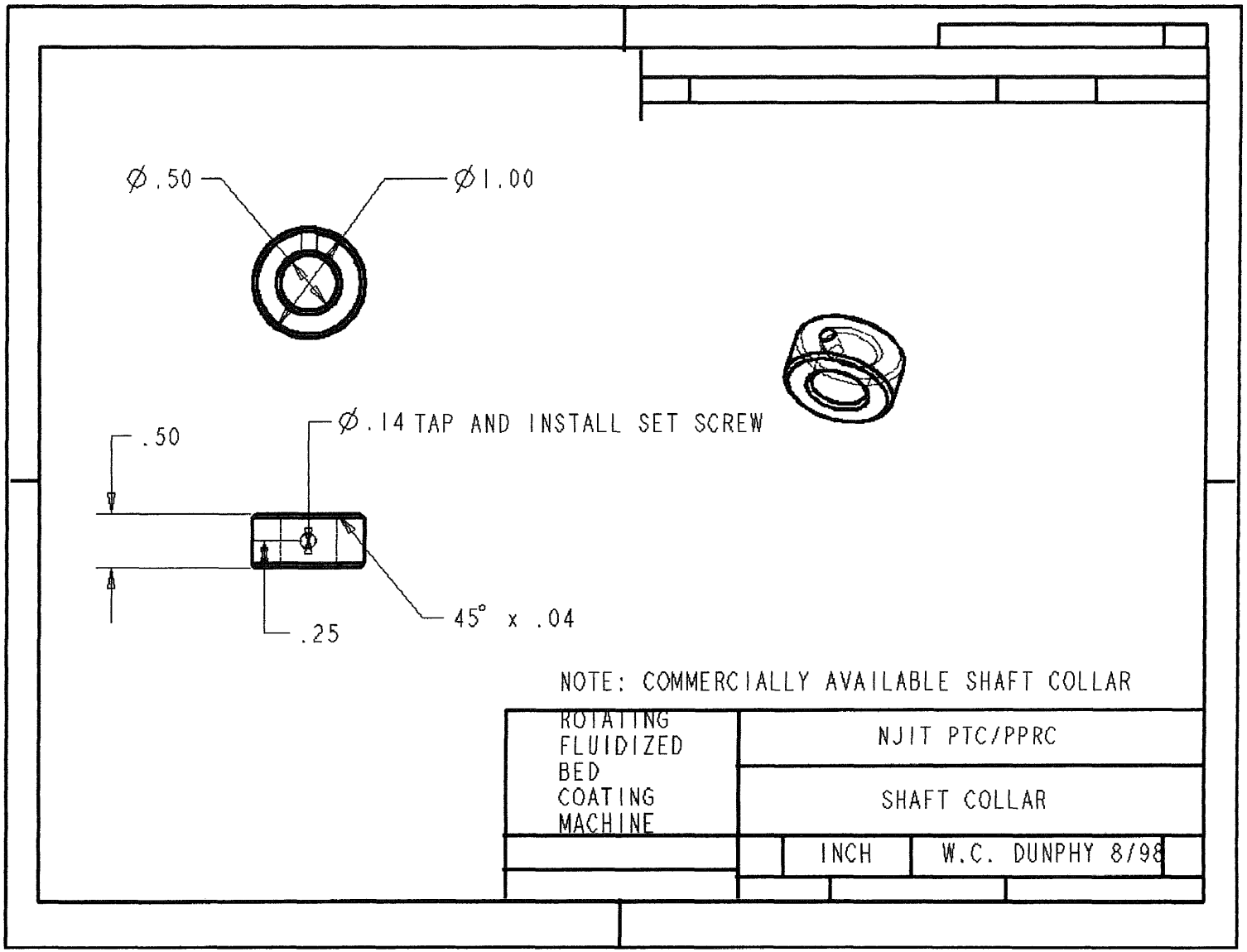

Fig A.7 shaft collar

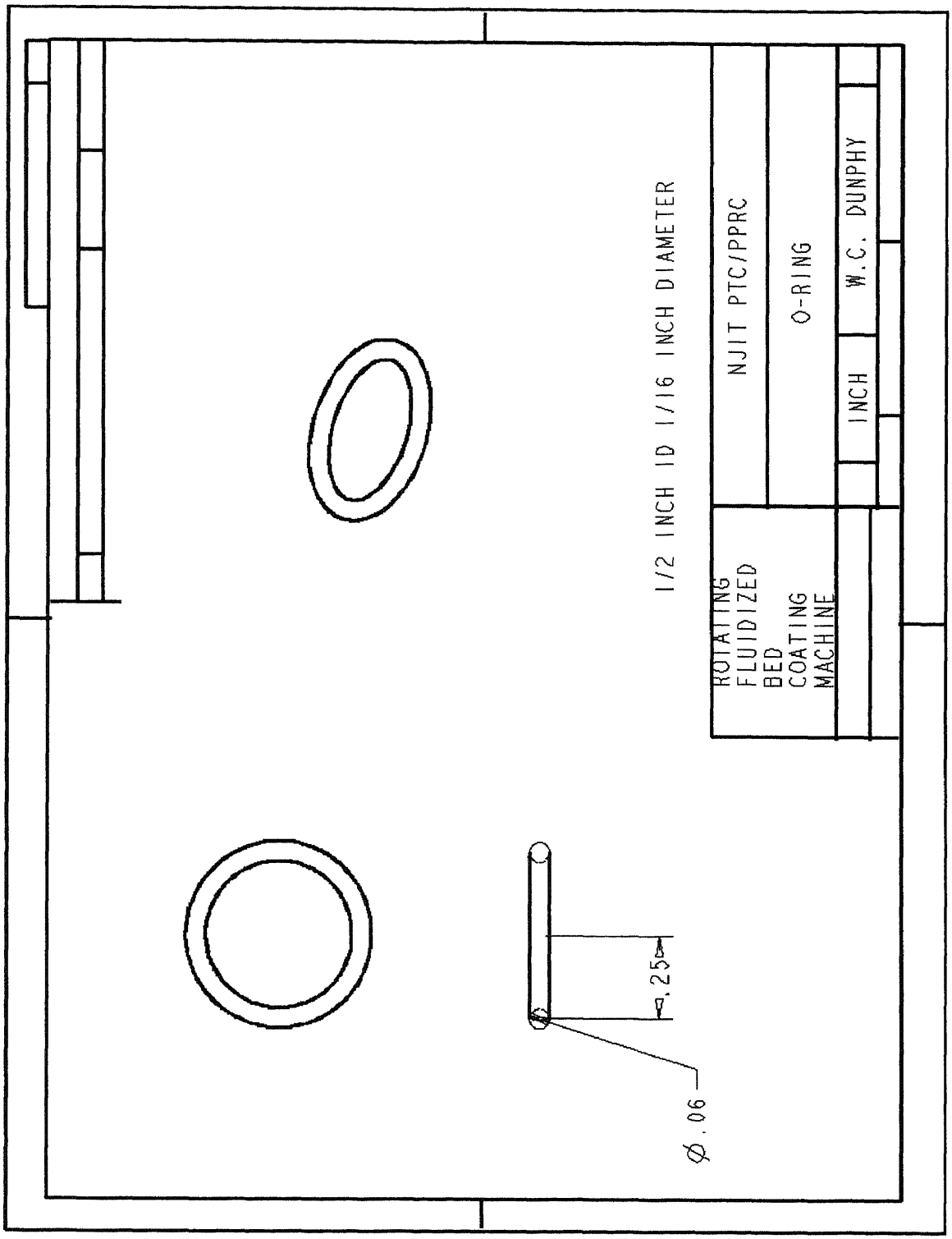
1/2 INCH ID 1/16 INCH DIAMETER
NJIT PTC/PPRC
O-RING
W.C. DUNPHY
INCH
ROTATING FLUIDIZED BED COATING MACHINE
.25
Ø.06

Fig A.8 o-ring

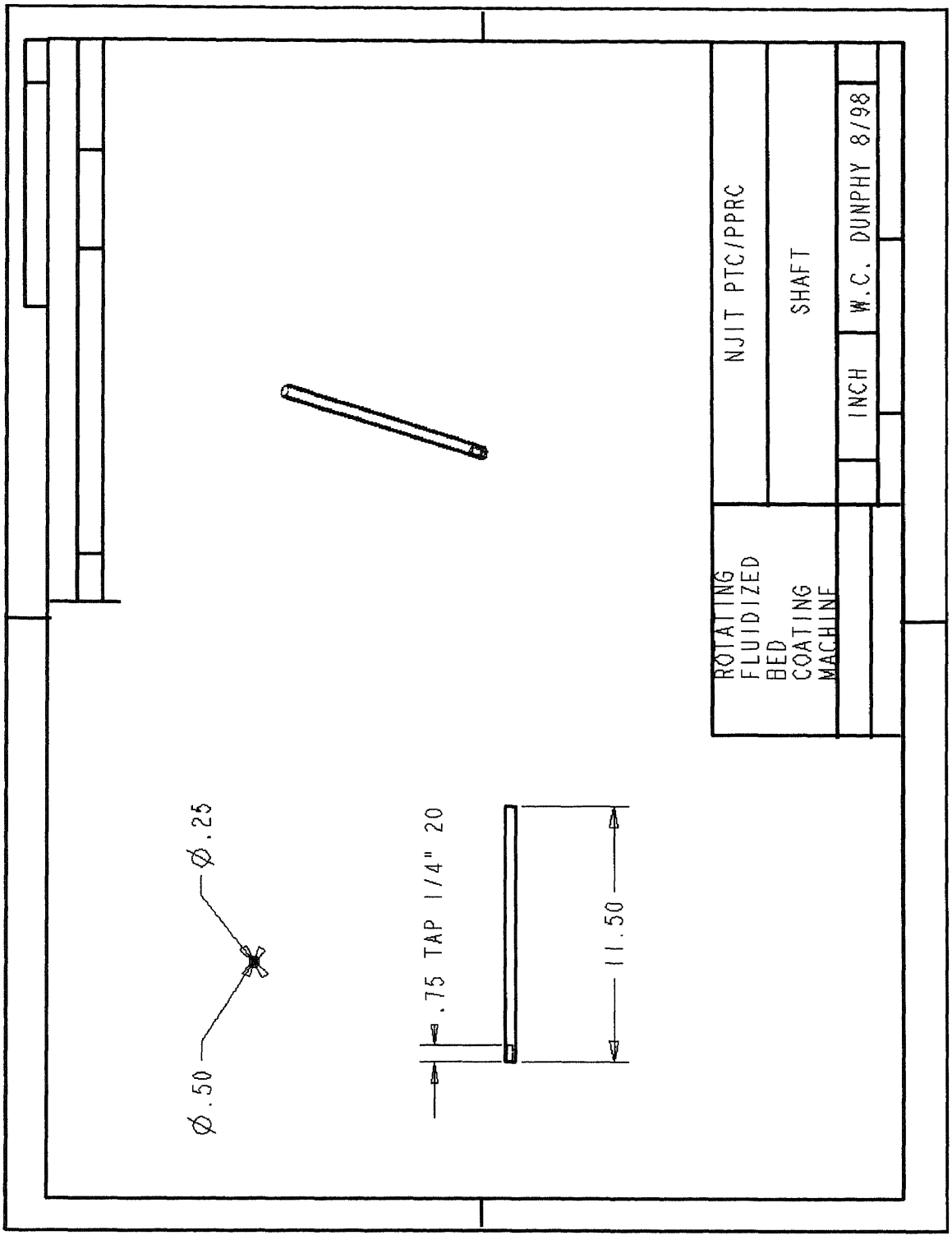
NJIT PTC/PPRC
SHAFT
W.C. DUNPHY 8/98
INCH
ROTATING
FLUIDIZED
BED
COATING
MACHINE
Ø.25
Ø.50
.75 TAP 1/4" 20
11.50

Fig A.9 shaft

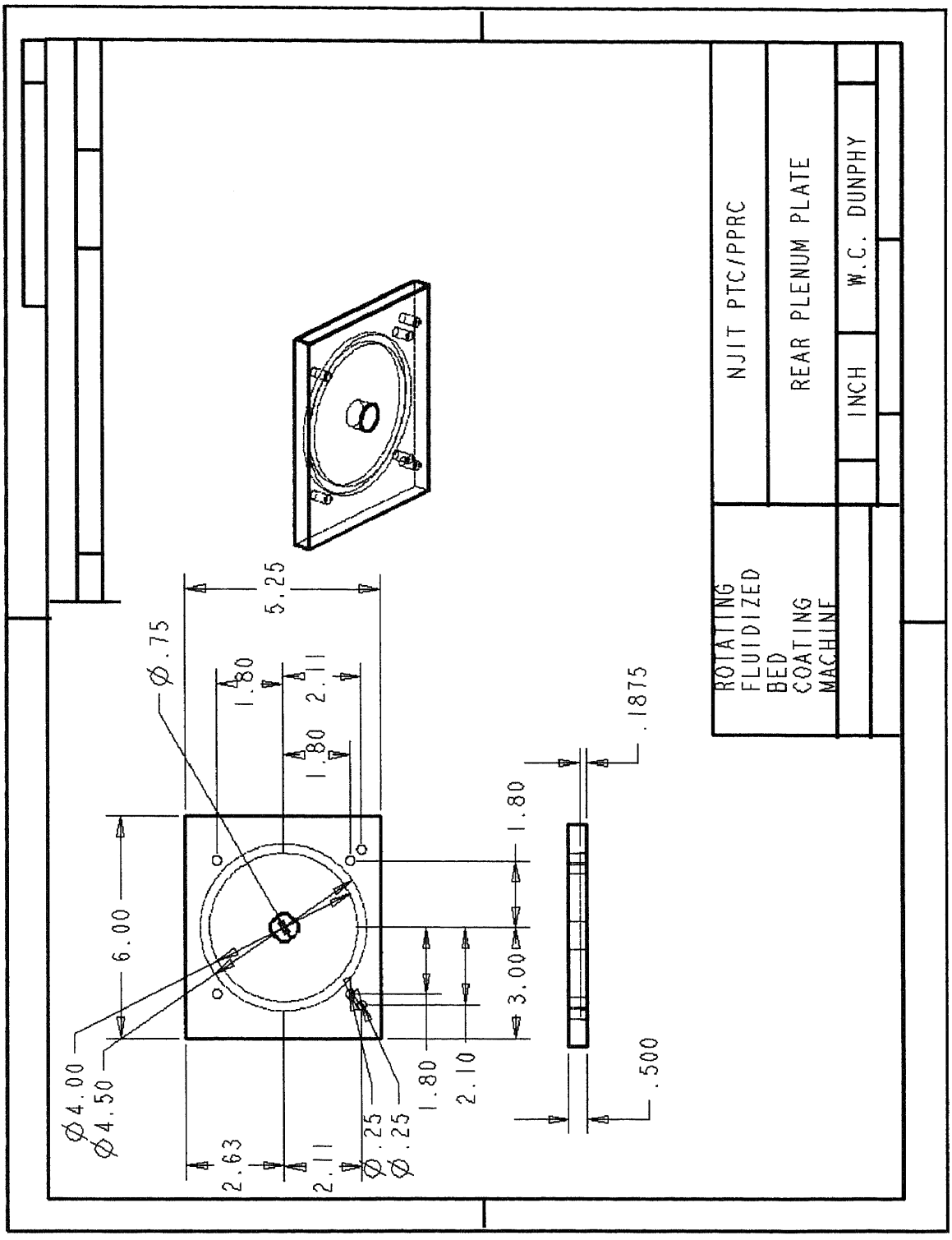

Fig A.10 rear plenum plate

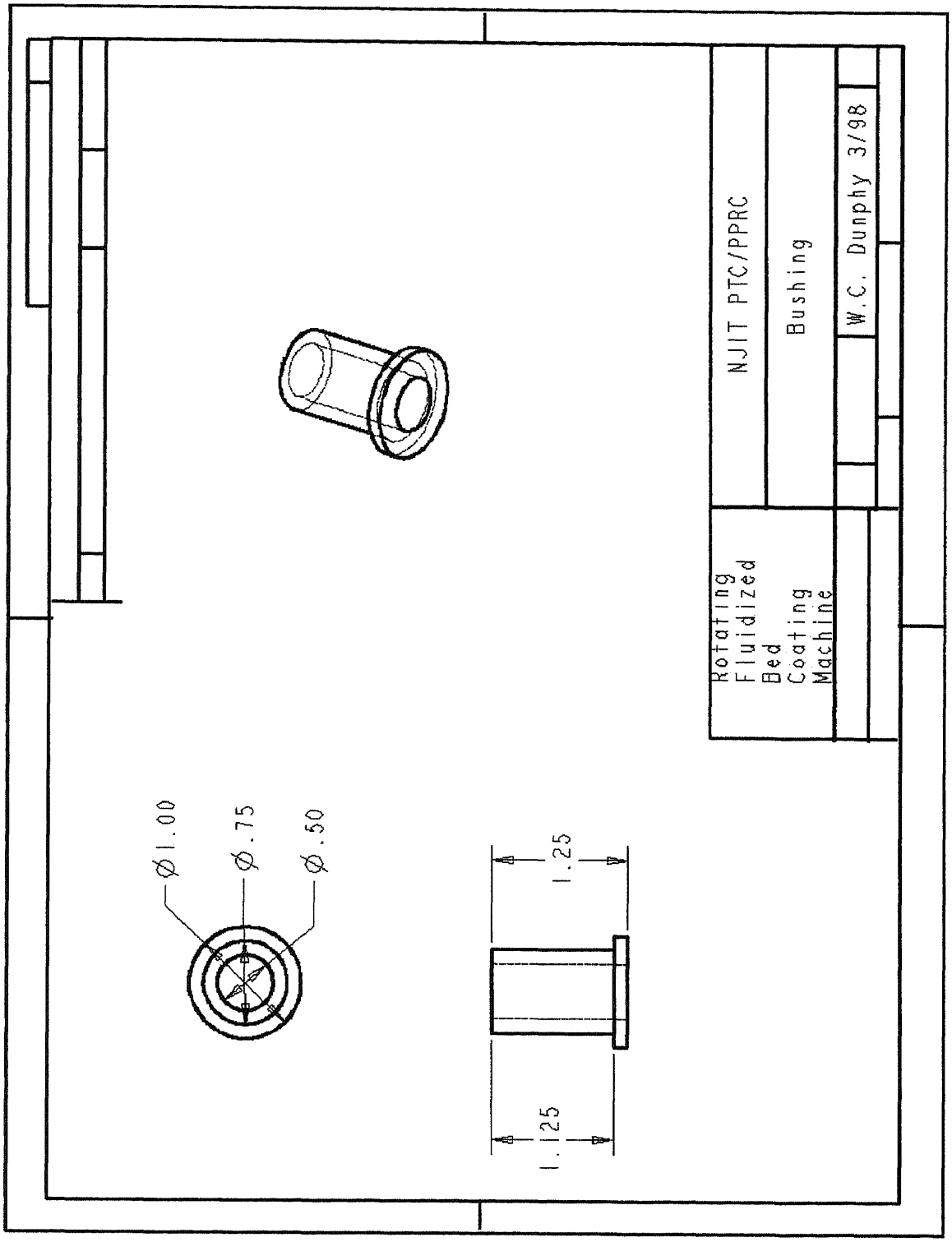

Fig A.11 bushing

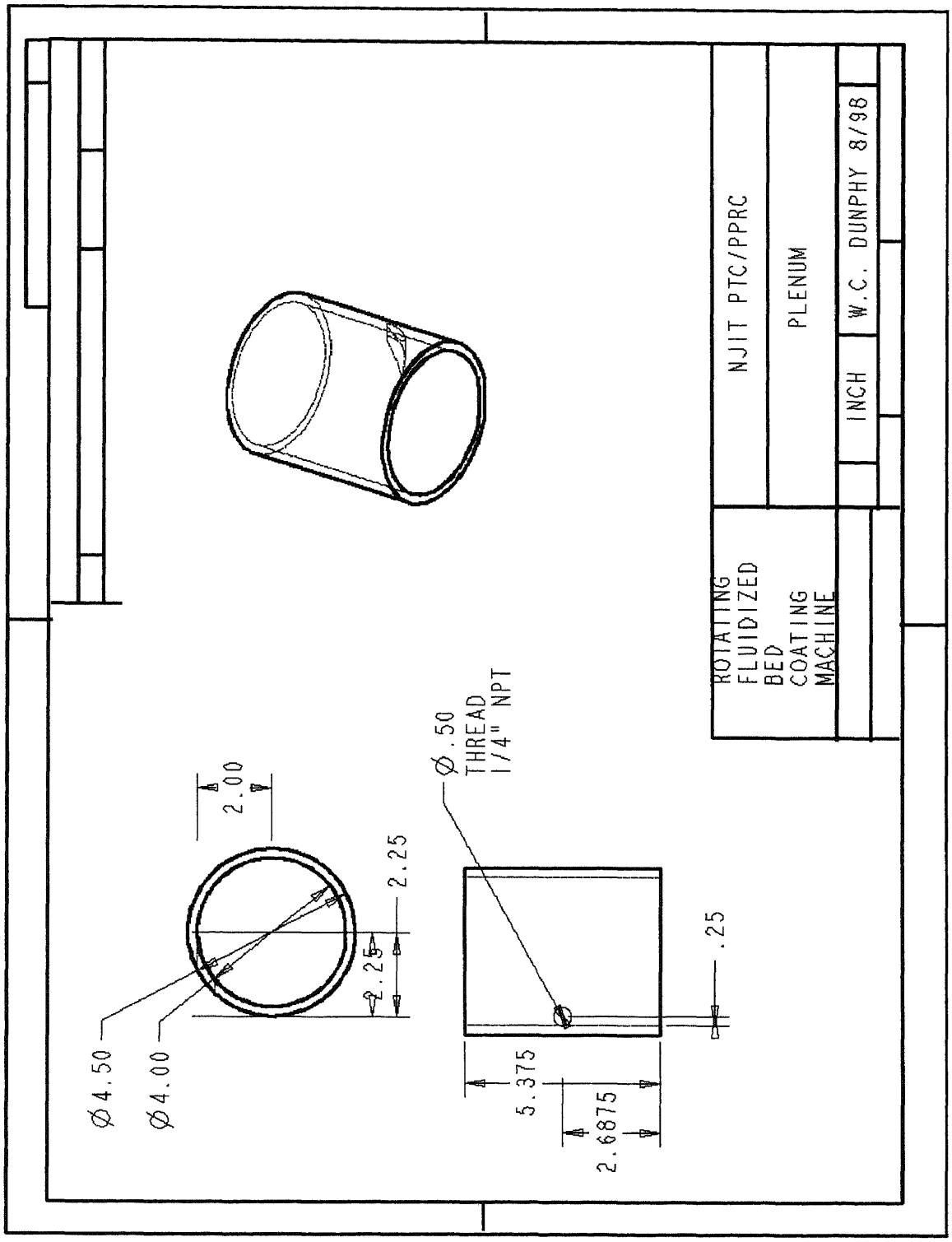

Fig A.12 plenum

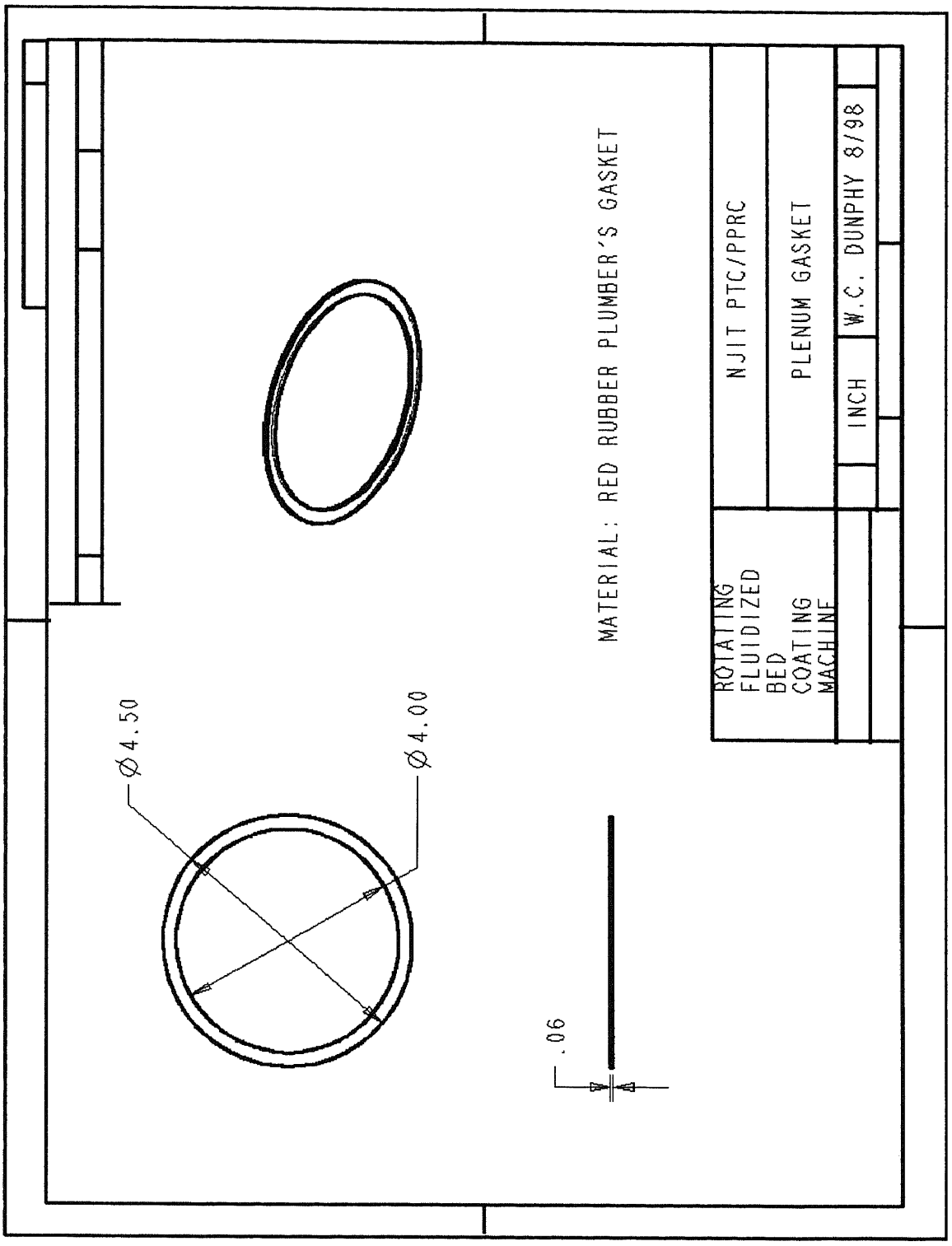

Fig A.13 plenum gasket

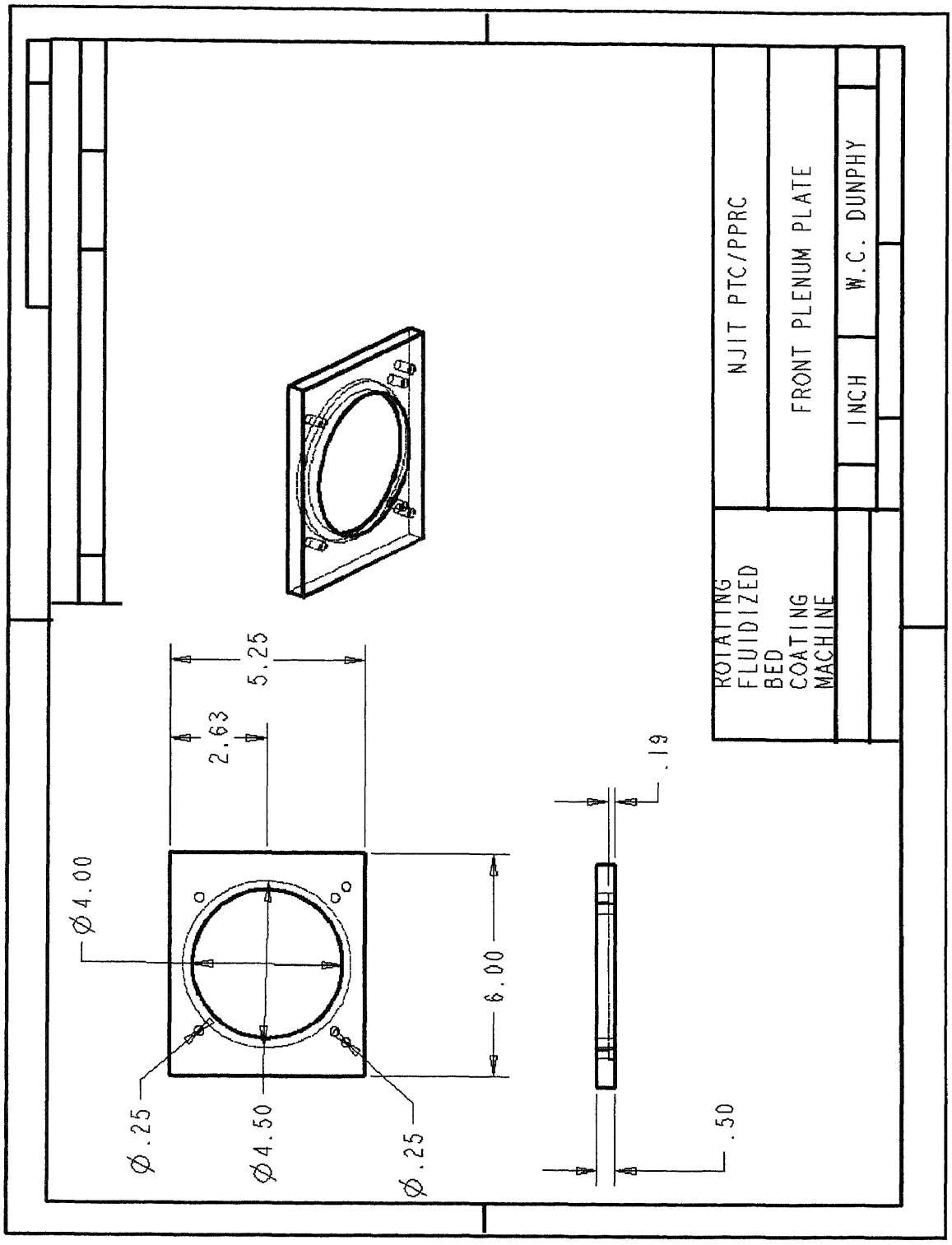

Fig A.14 front plenum plate

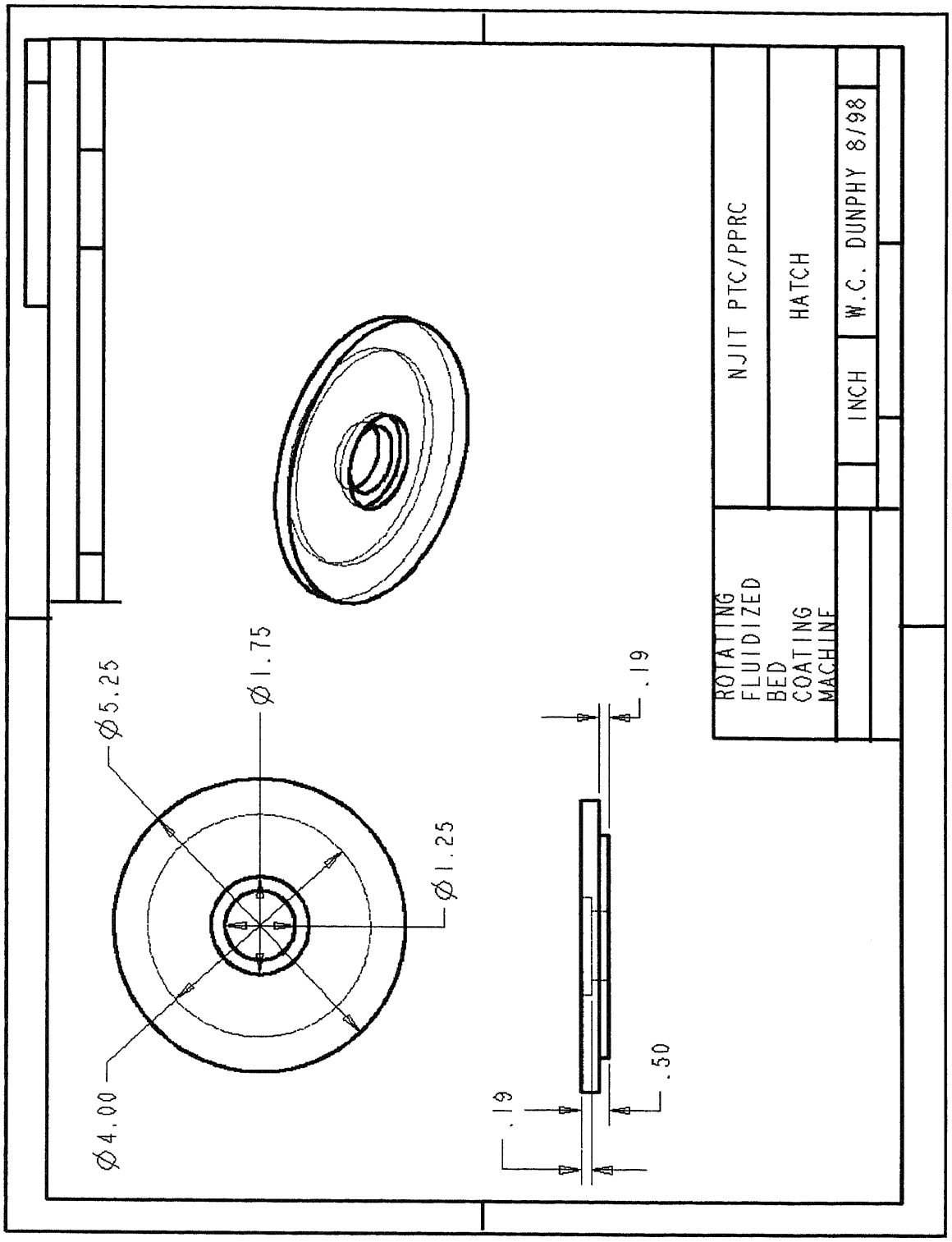

Fig A.15 hatch

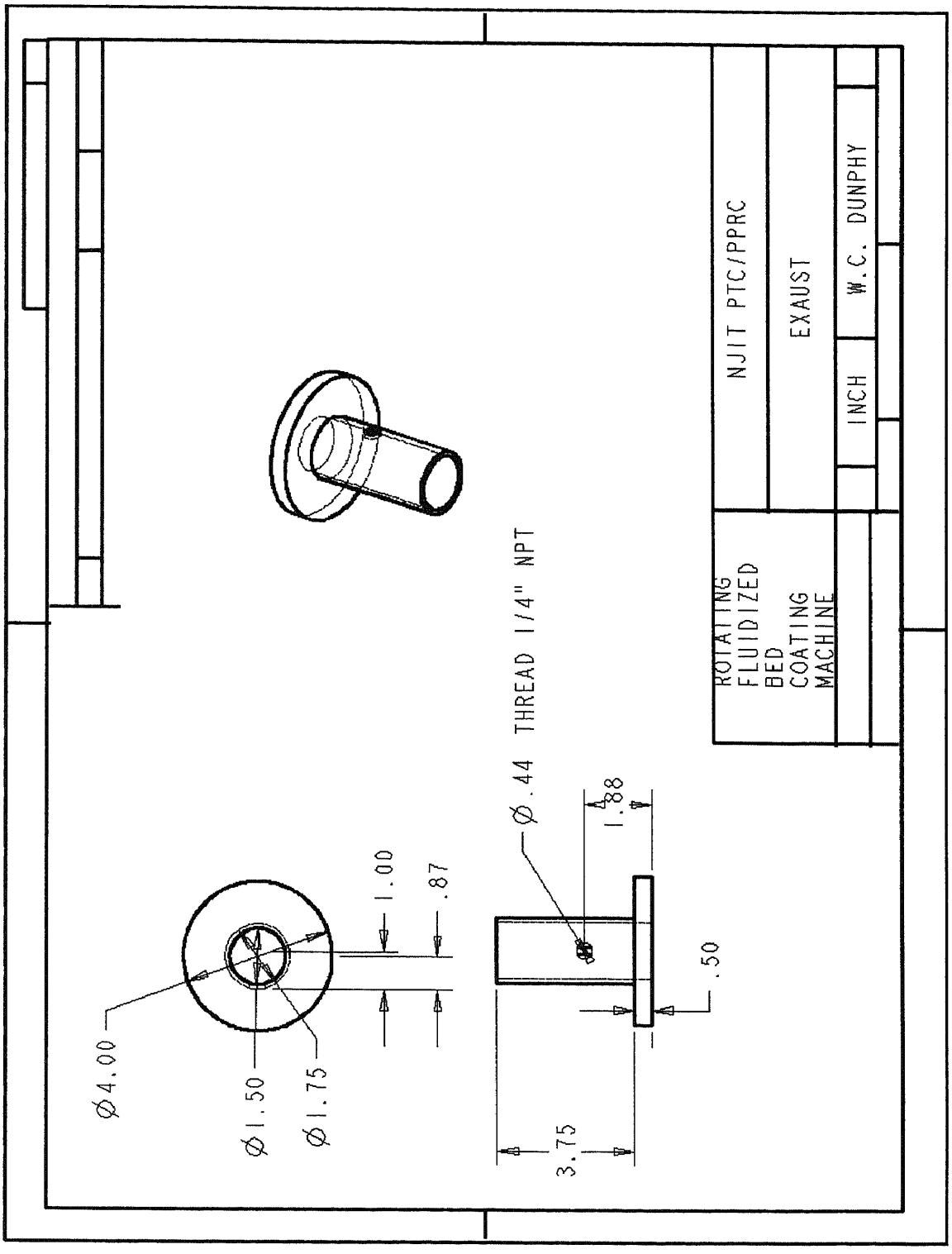

Fig A.16 exaust

APPENDIX B

S.E.M. IMAGES

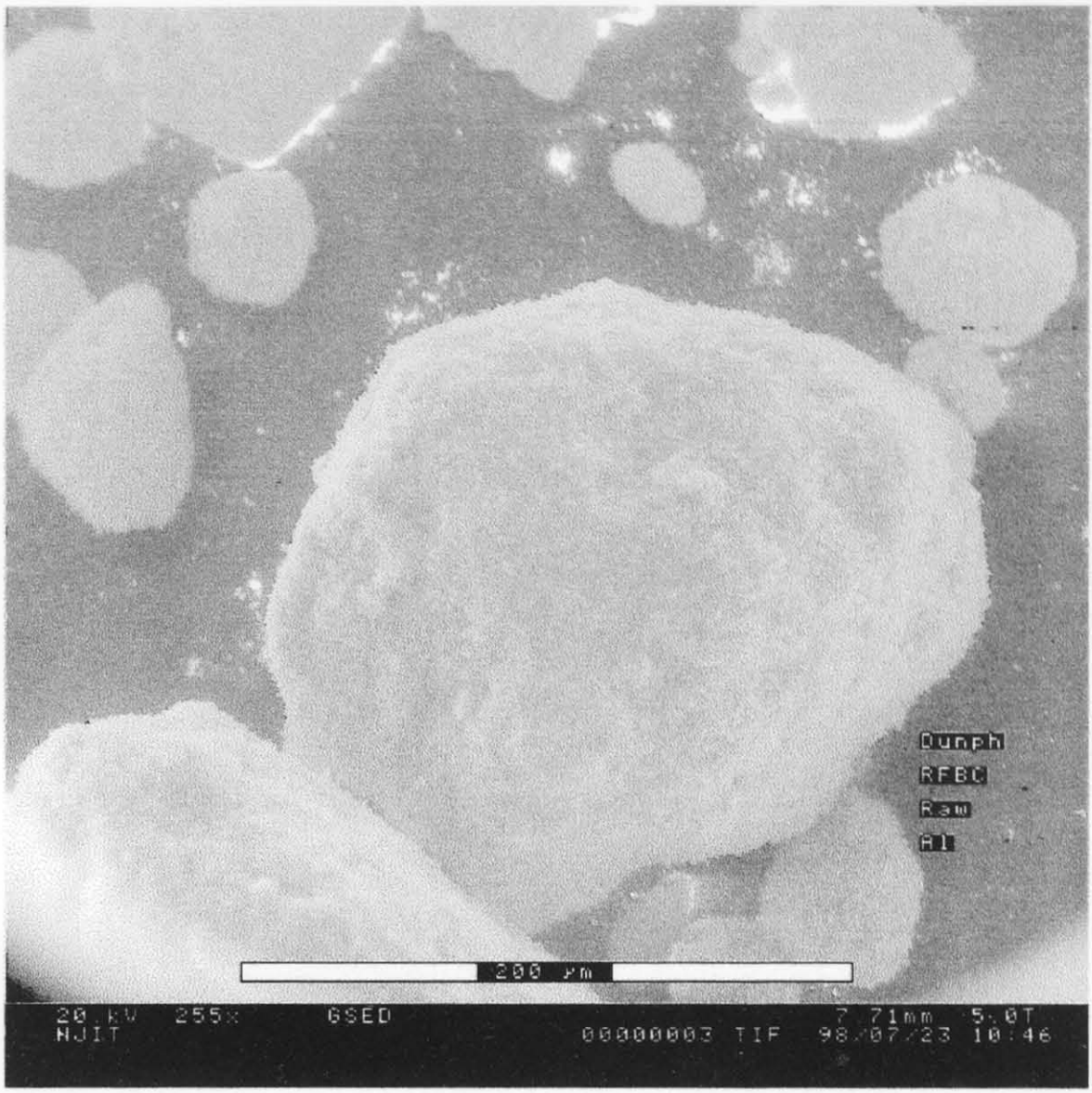

Fig B.1 raw alumina SEM

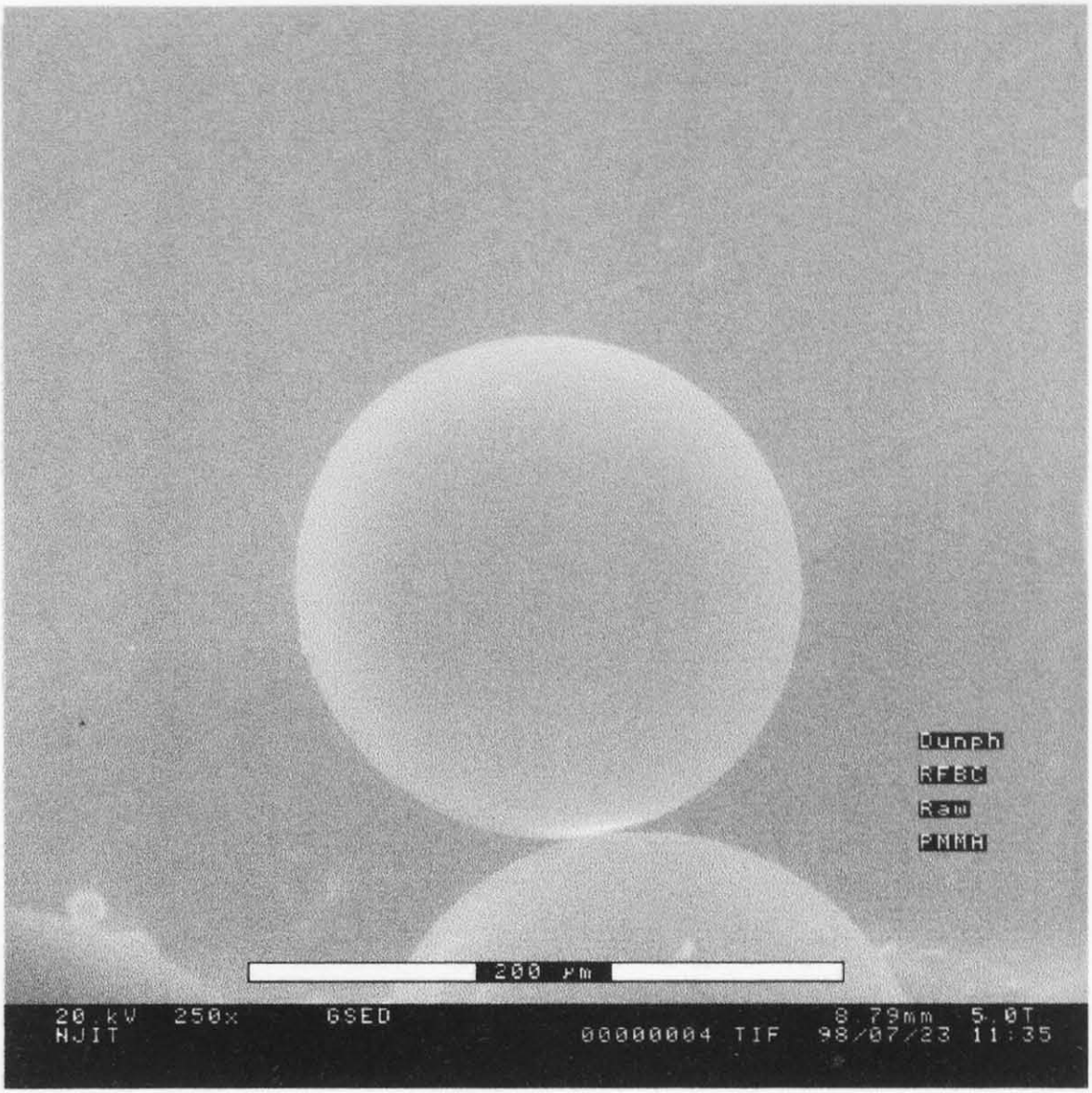

Fig B.2 raw PMMA SEM

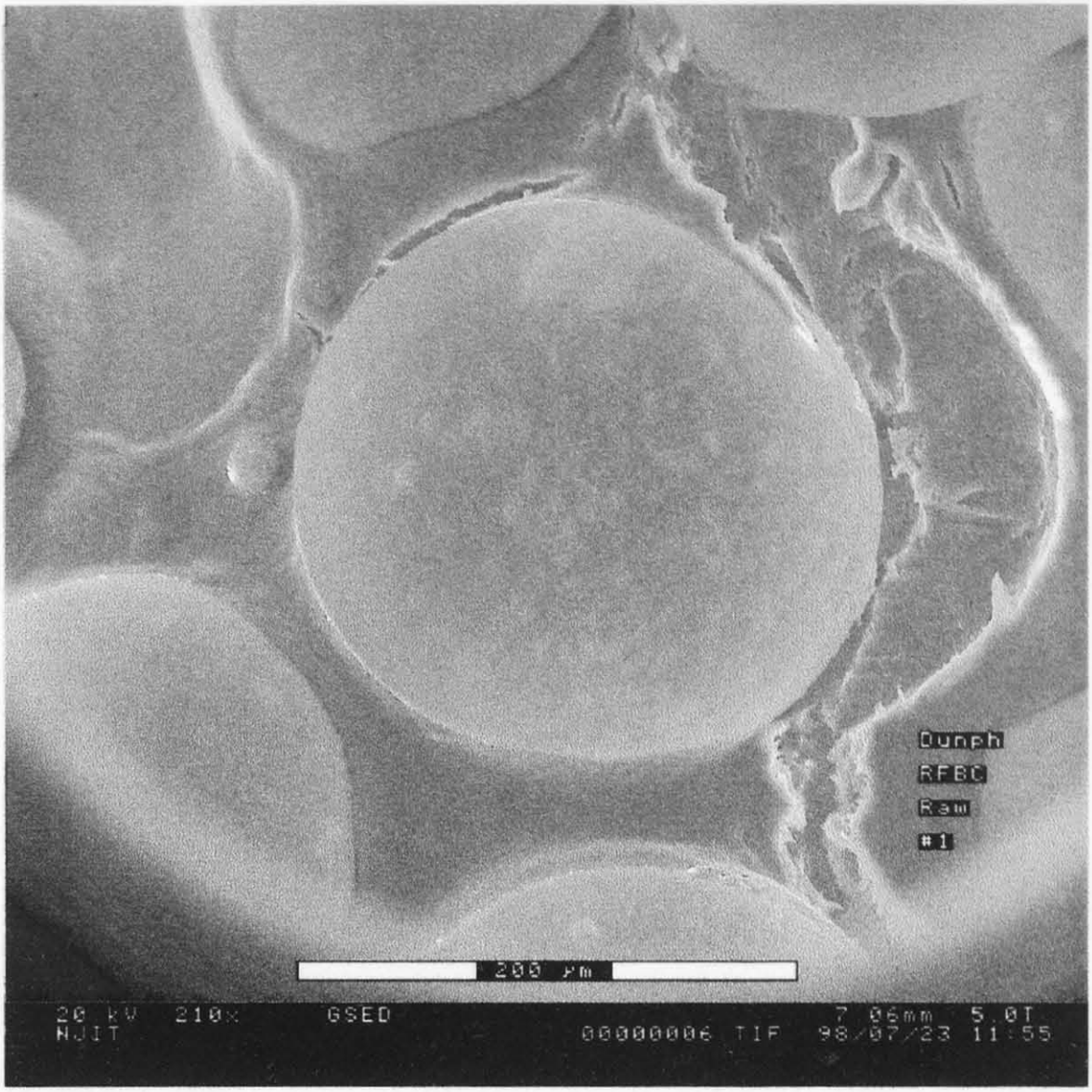

Fig B.3 sample #1 raw SEM

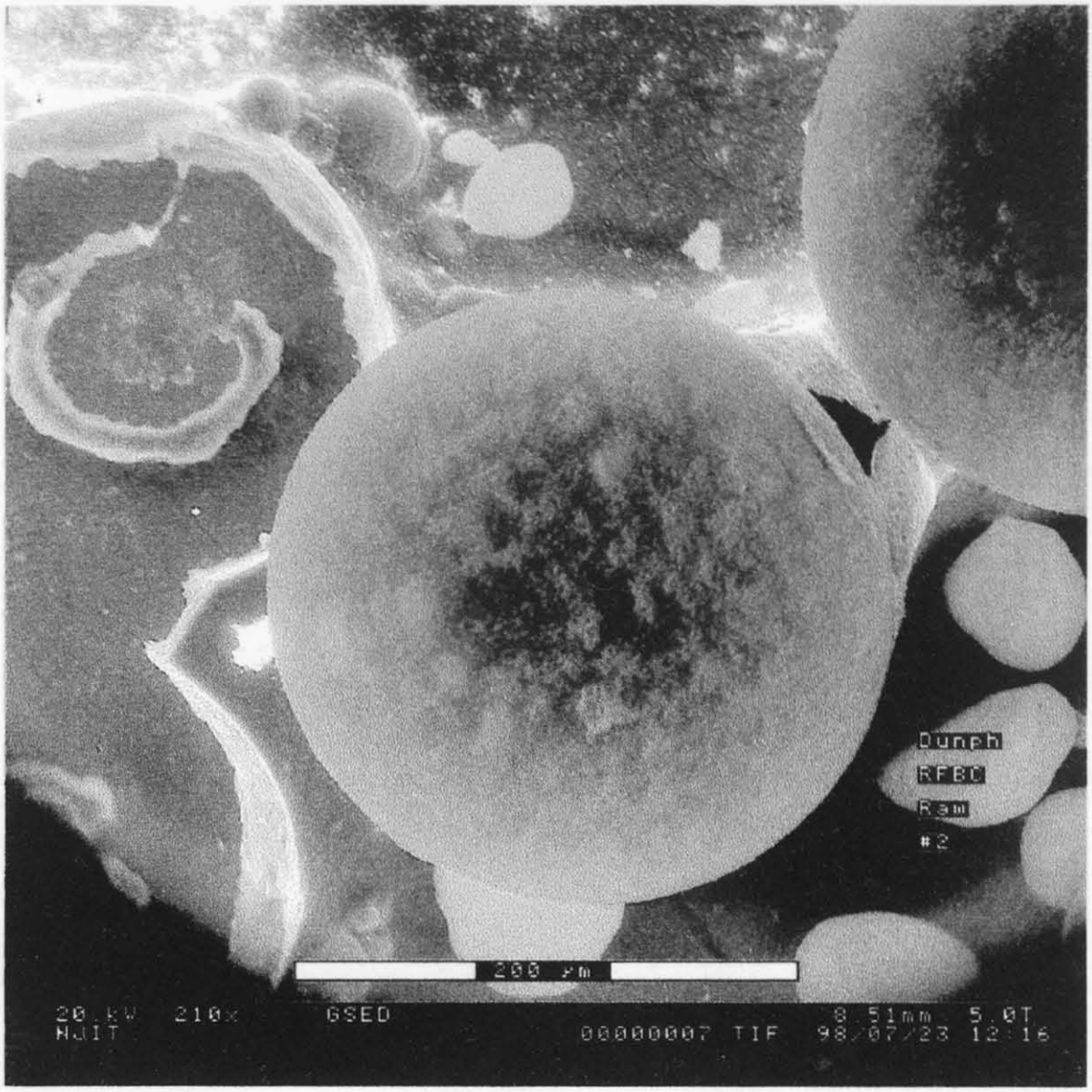

Fig B.4 sample #2 raw SEM

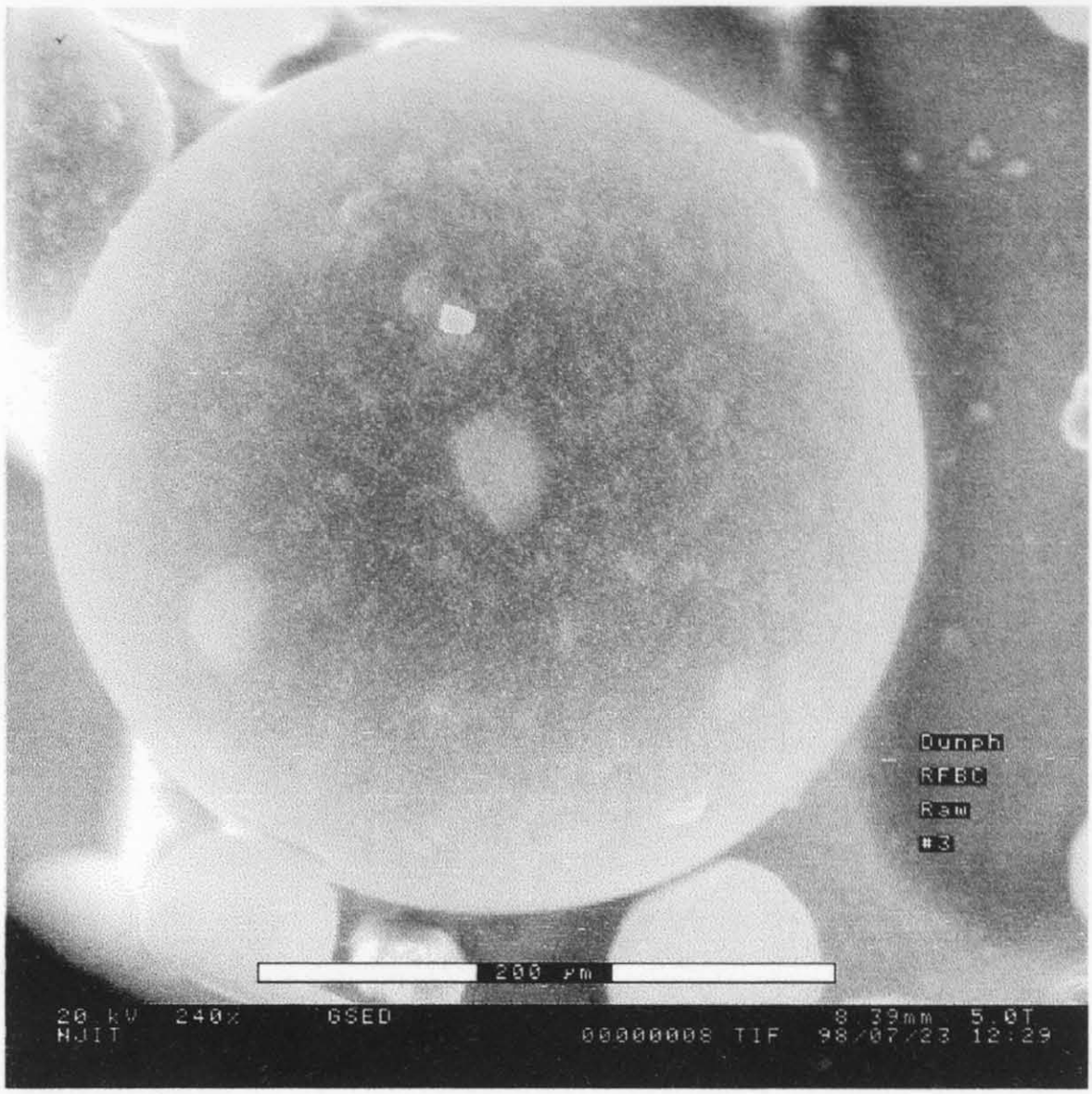

Fig B.5 sample #3 raw SEM

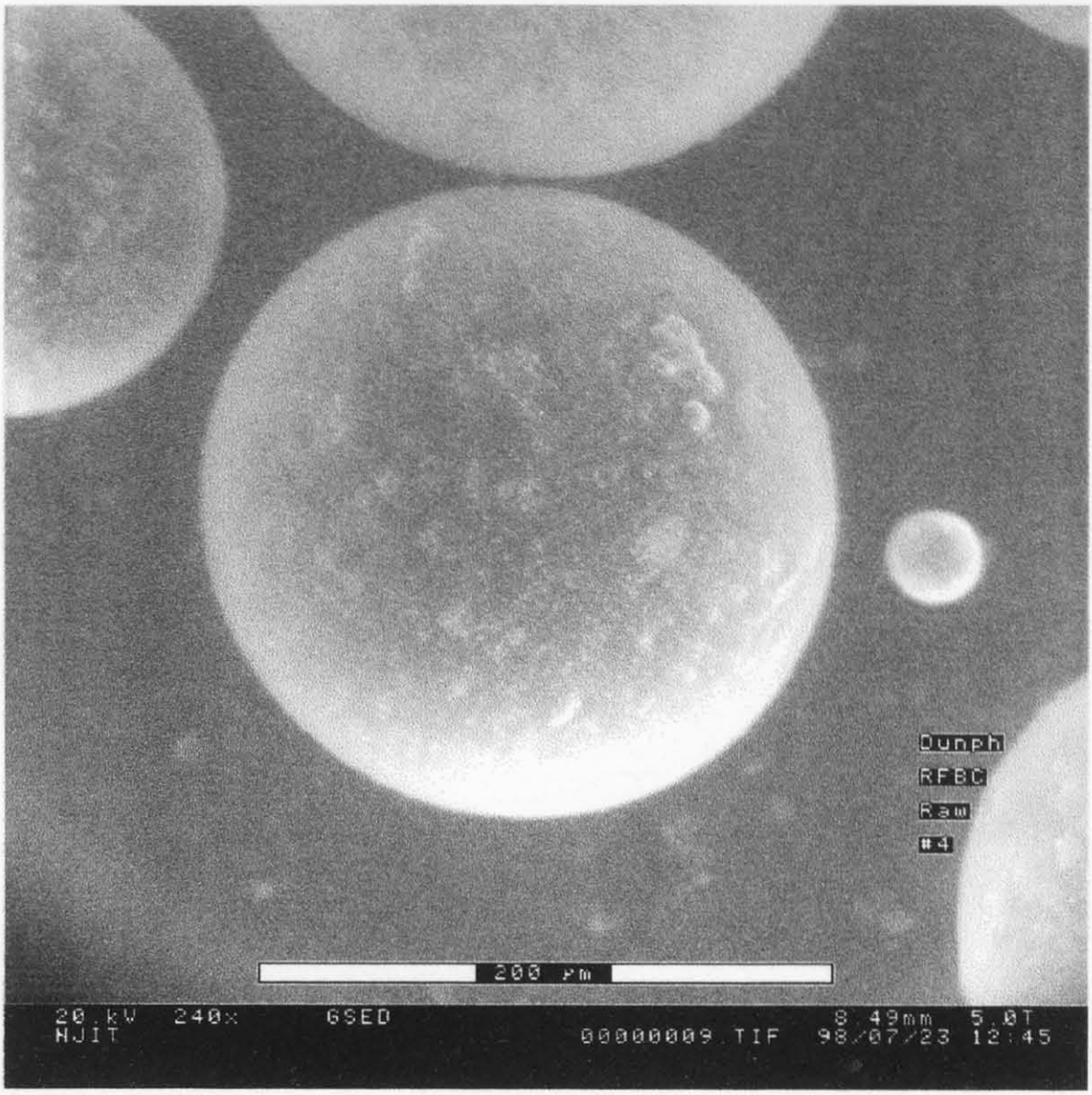

Fig B.6 sample #4 raw SEM

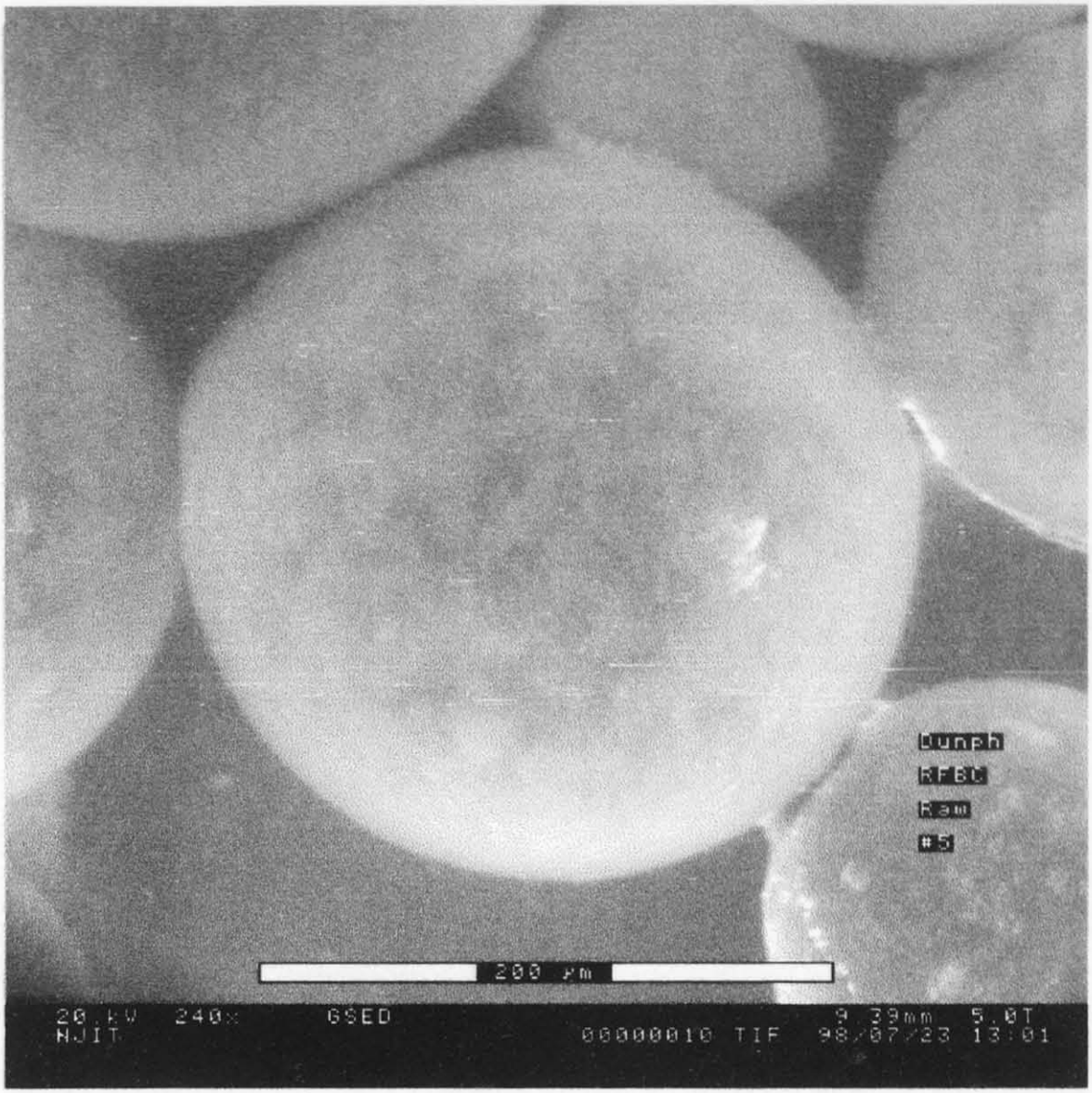

Fig B.7 sample #5 raw SEM

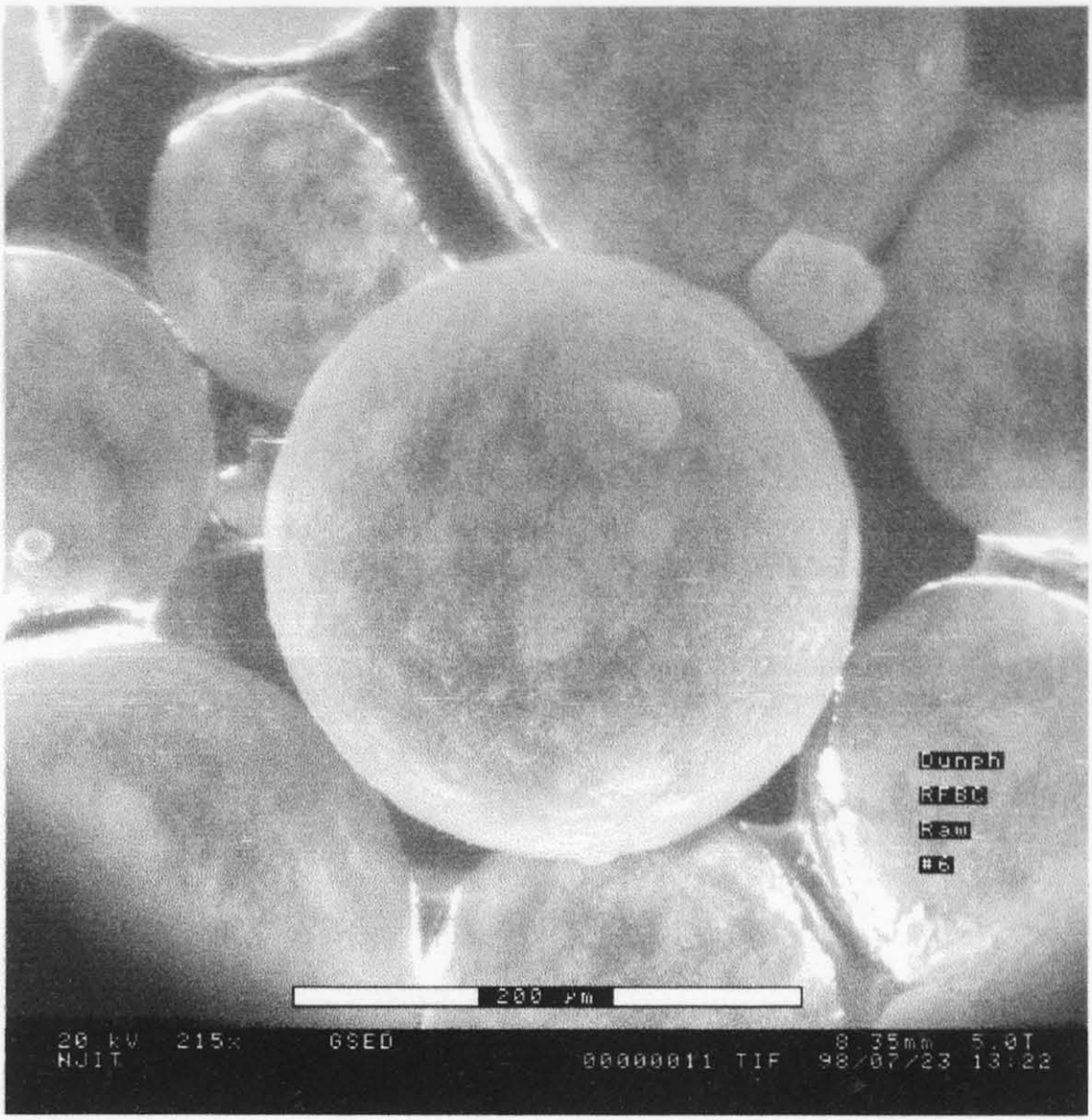

Fig B.8 sample #6 raw SEM

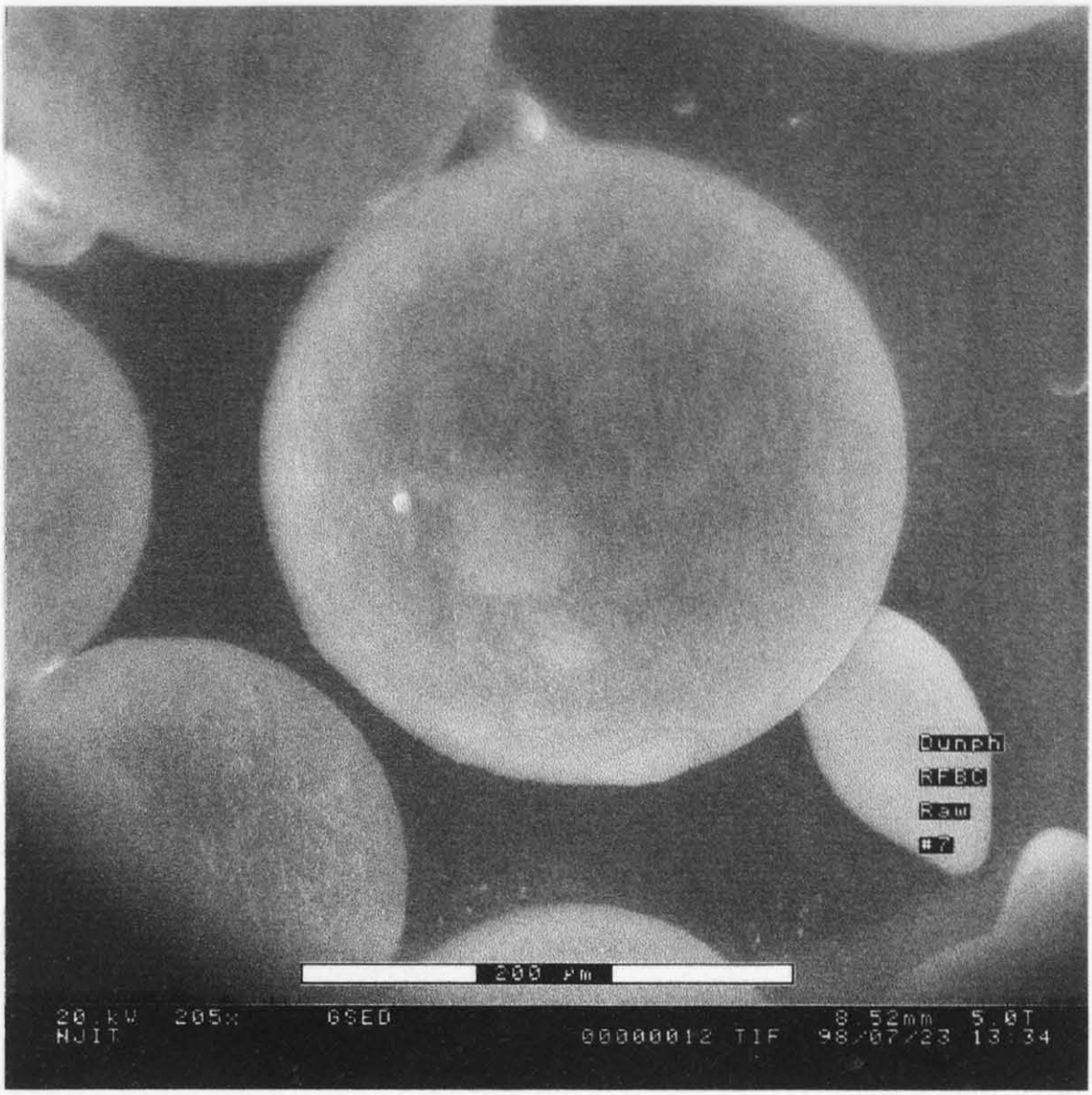

Fig B.9 sample #7 raw SEM

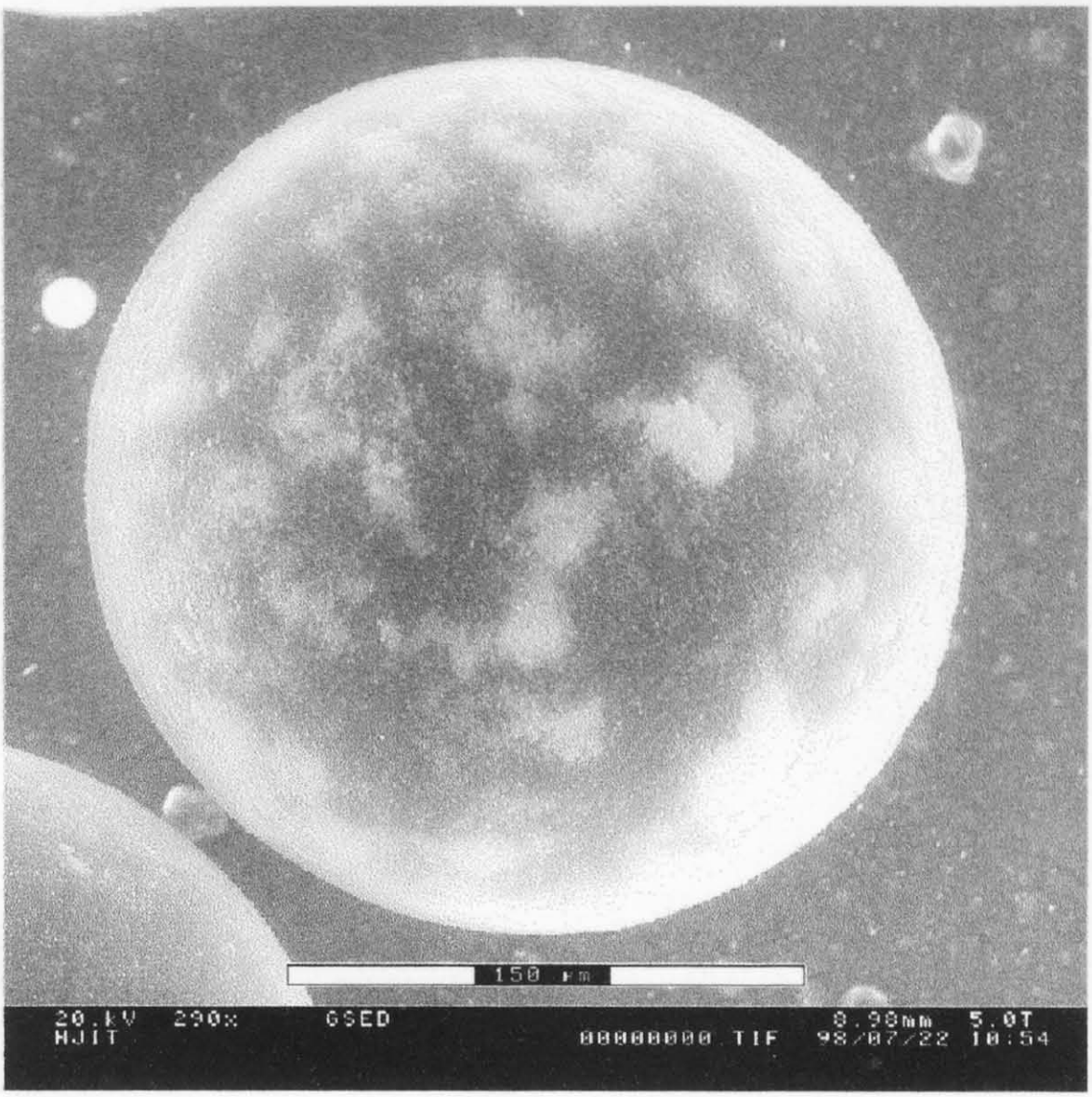

Fig B.10 sample #12 raw SEM

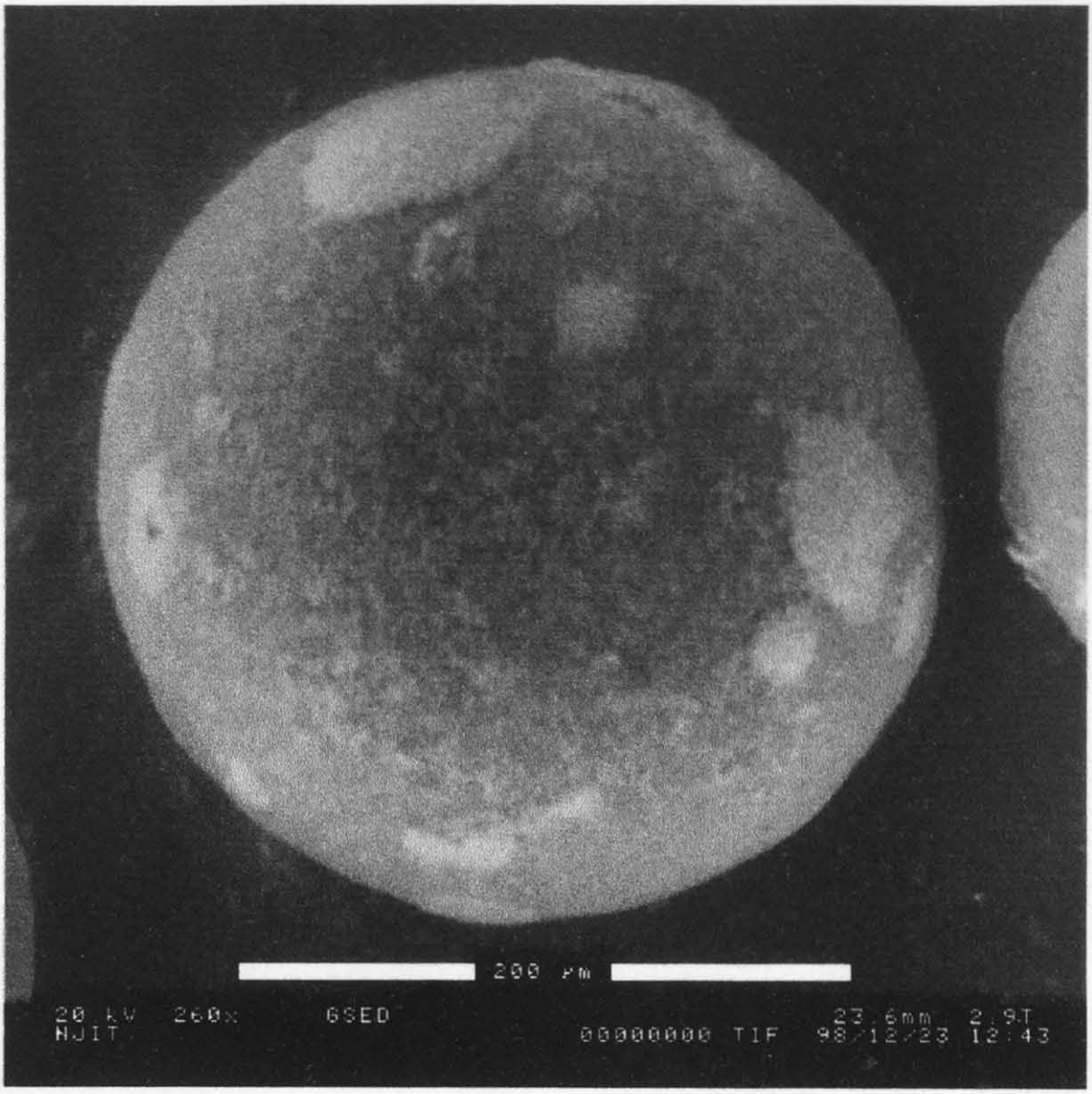

Fig B.11 sample #10 sonicated SEM

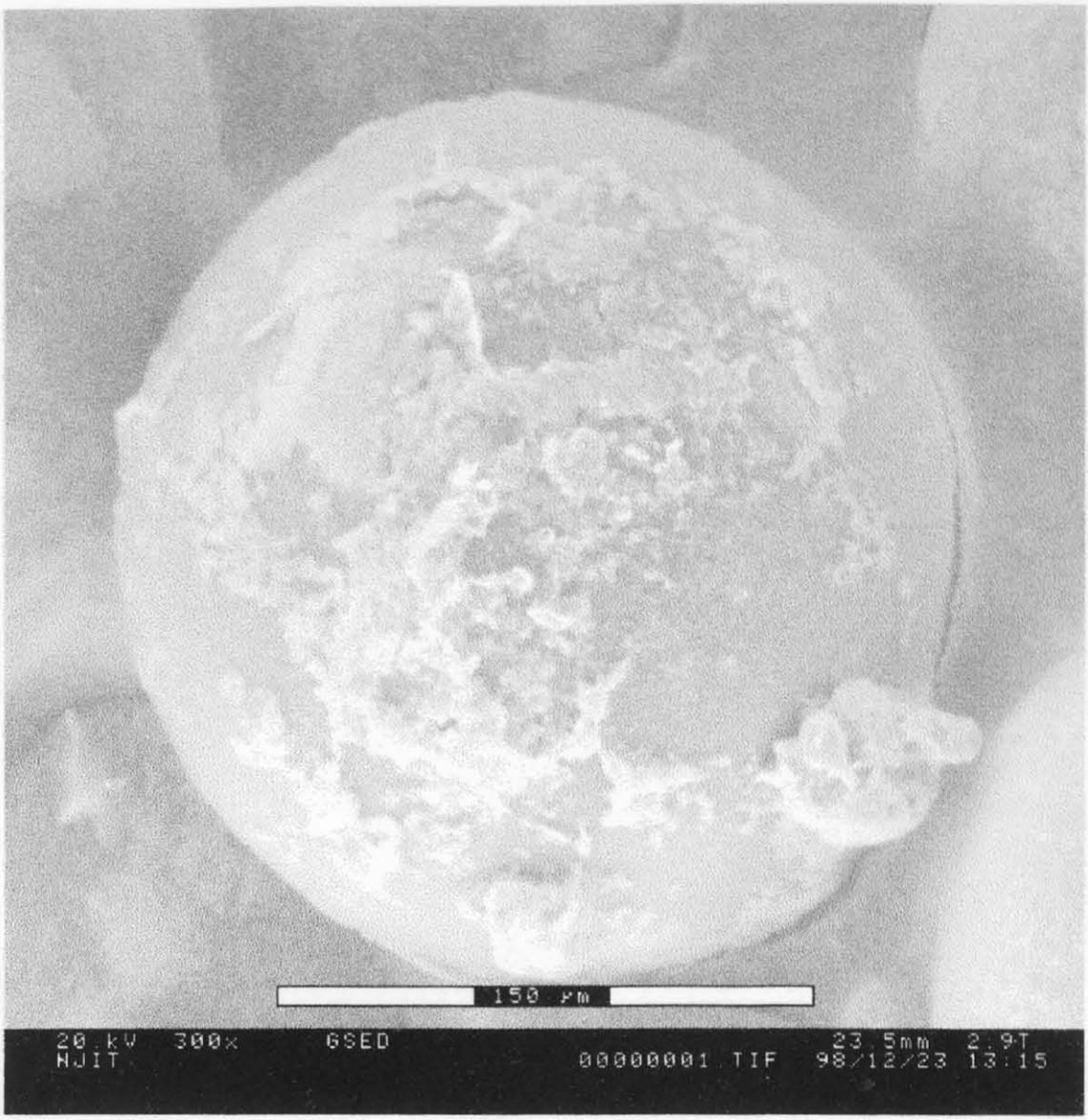

Fig B.12 sample #11 sonicated SEM

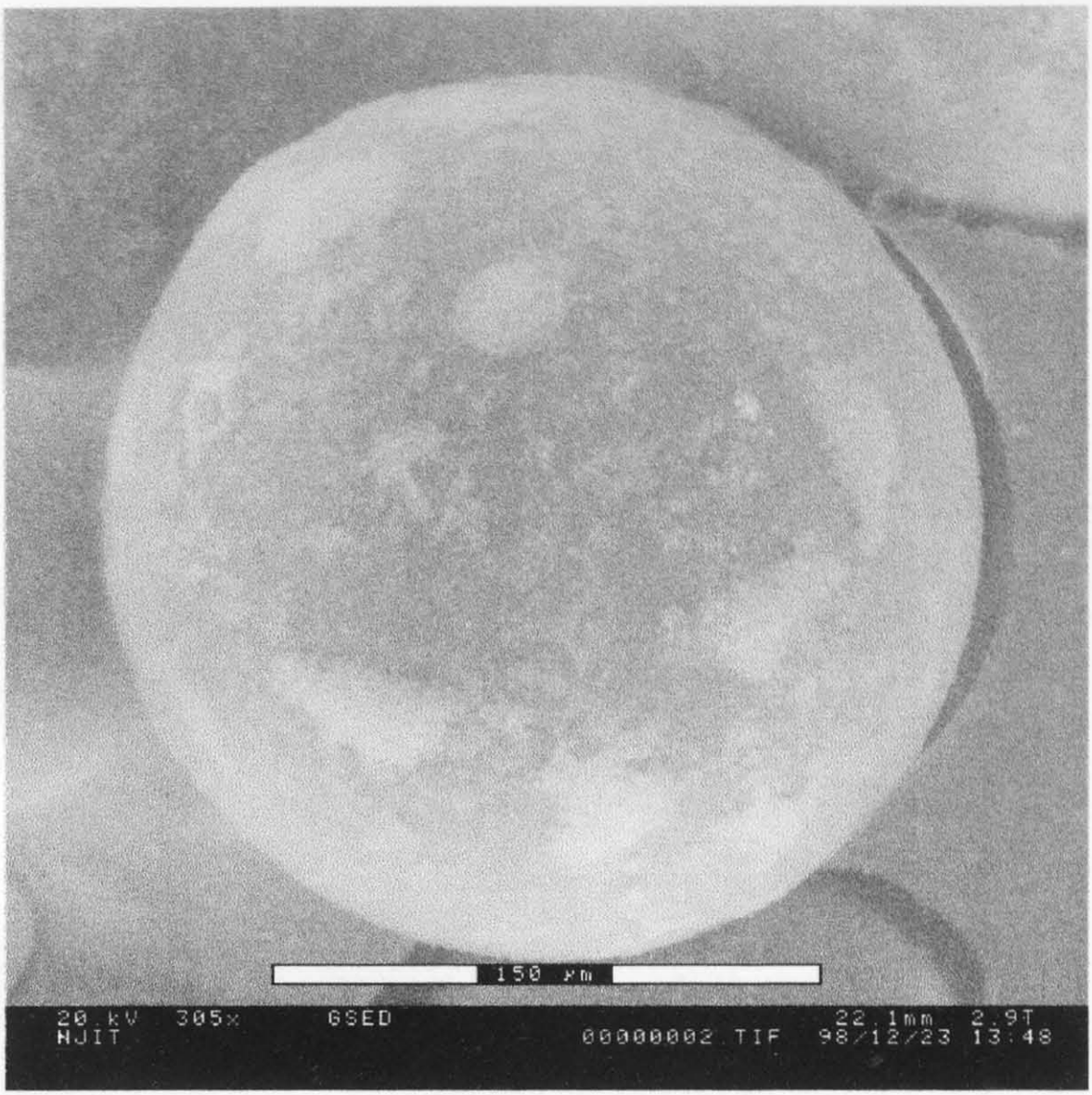

Fig B.13 sample #12 sonicated SEM

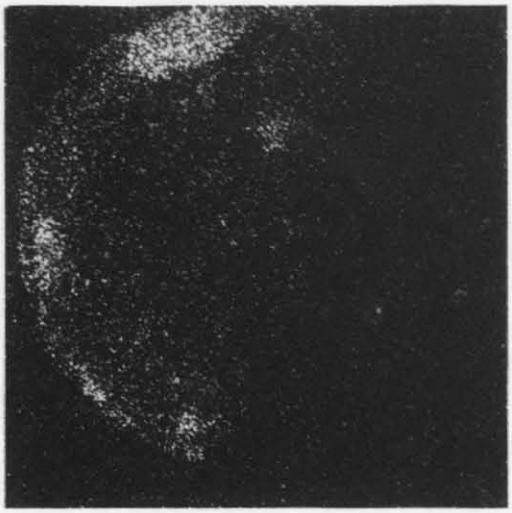

Fig B.14 sample #10 sonicated EDX Al

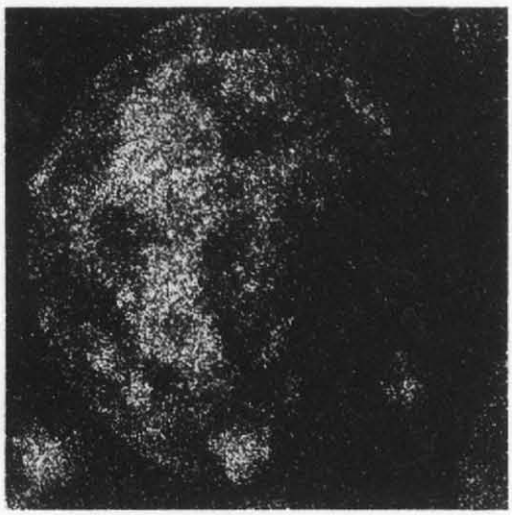

Fig B.15 sample #11 sonicated EDX Al

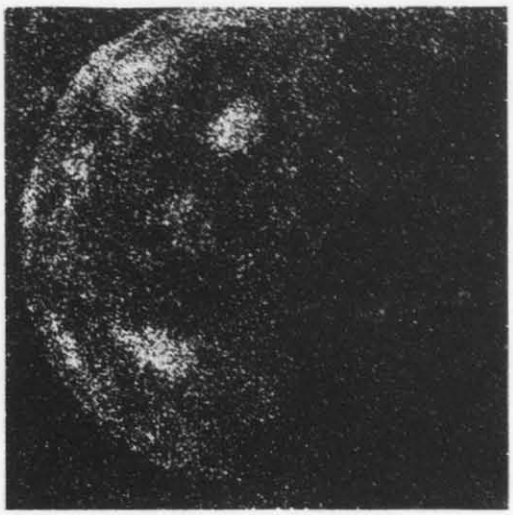

Fig B.16 sample #12 sonicated EDX Al

APPENDIX C

DERIVATION OF FLUIDIZATION EQUATIONS

Taken from [1]

In the fixed bed region the pressure drop is given by the Ergun equation,

$$\frac{dP}{dr} = \phi_1\left(\frac{U_o r_o}{r}\right) + \phi_2\left(\frac{U_o r_o}{r}\right)^2 + \rho_f r\omega^2 + \frac{\rho_f U_o^2 r_o^2}{\varepsilon^2 r^3}$$

where;

$$\phi_1 = \frac{150(1-\varepsilon)^2\mu}{\varepsilon^3(\phi_s d_g)^2}; \phi_2 = \frac{1.75(1-\varepsilon)\rho_f}{\varepsilon^3\phi_s d_g}$$

in the fluidized bed region given by,

$$\frac{dP}{dr} = (\rho_g - \rho_f)(1-\varepsilon)r\omega^2 + \rho_f \varepsilon r\omega^2 + \frac{\rho_f U_o^2 r_o^2}{\varepsilon r^3} + \frac{\rho_f U_o^2 r_o^2}{\varepsilon^2 r^2}\frac{d\varepsilon}{dr}$$

however; in the fixed bed region the major contribution is from the drag force per unit volume, while in the fluidized bed region the major contribution is from the total mass of particles, therefore the above equations reduce to;

$$\frac{dP}{dr} = \phi_1\left(\frac{U_o r_o}{r}\right) + \phi_2\left(\frac{U_o r_o}{r}\right)^2$$

in the fixed bed region and to

$$\frac{dP}{dr} = (\rho_g - \rho_f)(1-\varepsilon)r\omega^2$$

in the fluidized bed region. Integrating the above equations from r_i to r_o results in;

$$\frac{U_{mf}\rho_f d_g}{\mu} = \left[\left(33.7\frac{C_2}{C_1}\right)^2 + 0.0408\frac{\rho_f(\rho_g - \rho_f)d_g^3\omega^2}{\mu^2}\frac{C_3}{C_1}\right]^{1/2} - 33.7\frac{C_2}{C_1}$$

where;

$$C_1 = r_\infty^2\left(1/r_i - 1/r_o\right)$$

$$C_2 = r_\infty \ln\left(r_o/r_i\right)$$

$$C_3 = \left(r_o^2 - r_i^2\right)/2$$

As we are not concerned with average fluidization velocity within the scope of this thesis, we will evaluate the above equation at $r = r_o$ and introduce U_{mfc} where the whole bed is fluidized, the result is;

$$\frac{U_{mfc}\rho_f d_g}{\mu} = \left[(33.7)^2 + 0.0408\frac{\rho_f\left(\rho_g - \rho_f\right)d_g^3\omega^2 r_o}{\mu^2}\right]^{1/2} - 33.7$$

it is at this point that the partial fluidization graph joins the full fluidization graph, partial fluidization is given by;

$$\Delta P = (1-\varepsilon)\left(\rho_g - \rho_f\right)\omega^2\left(r_{pf}^2 - r_i^2\right) + \phi_1 U_o r_o \ln\left(r_o/r_{pf}\right) + \phi_2 U_o^2 r_o^2\left(1/r_{pf} - 1/r_o\right)$$

where r_{pf} is the interface of the fluidized and packed beds, full fluidization is given by;

$$\Delta P_f = (1-\varepsilon)\left(\rho_g - \rho_f\right)\omega^2\left(r_o^2 - r_i^2\right)/2$$

NOTATION

d_g = granule diameter

ΔP = total pressure drop across fluidized bed

ΔP_f = pressure drop across fluidized bed

r = radial coordinate

r_i = radius of inner surface of granule bed

r_o = radius of rotating fluidized bed

r_{pf} = radius of interface between fluidized and packed bed

U_{mf} = average minimum fluidization velocity

U_{mfc} = critical minimum fluidization velocity

U_o = superficial air velocity based on outside radius

ε = void fraction

μ = air viscosity

ρ_f = air density

ρ_g = granule density

ω = angular velocity

APPENDIX D

INSTRUMENTATION OF RFB

A. U-Tube Manometer

In order that the pressure drop across the bed be measured differentially, a Dwyer™ U tube manometer 1 meter in length was installed with one lead in the plenum and the other in the exhaust.

B. Air Flow Rotometers

In order that the superficial air velocity be measured an array of three rotometers was purchased from Dwyer™ spanning air flow from 0 SCFH to 1800 SCFH. *WARNING: THE METERS SELECTED ARE RATED FOR 35 PSI MAX. PRESSURE, DURING A PROPERLY CONDUCTED EXPERIMENT THE PRESSURES DO NOT RISE ABOVE THIS RATING, IF THE EXHAUST IS CLOSED OFF OR THE AIR HOSES ARE CONNECTED IMPROPERLY, AN EXPLOSION OF THE METERS OR THE PLENUM MAY RESULT.*

C. Motor Microcontroler

The Dayton™ DC motor is equipped with a microcontroller capable of 0 RPM to 1725 RPM in 1 RPM increments.

D. Miscellaneous Equipment

The compressed air was delivered by the native air compressor in the lab. 1/2 inch air lines from Coilhose® were required to deliver the desired rate of air flow. Exhaust was removed via 1 1/4 inch flexible tubing into the native fume hood

system in the lab. The nozzle runout was adjusted with the use of a Starret® dial indicator and stand.

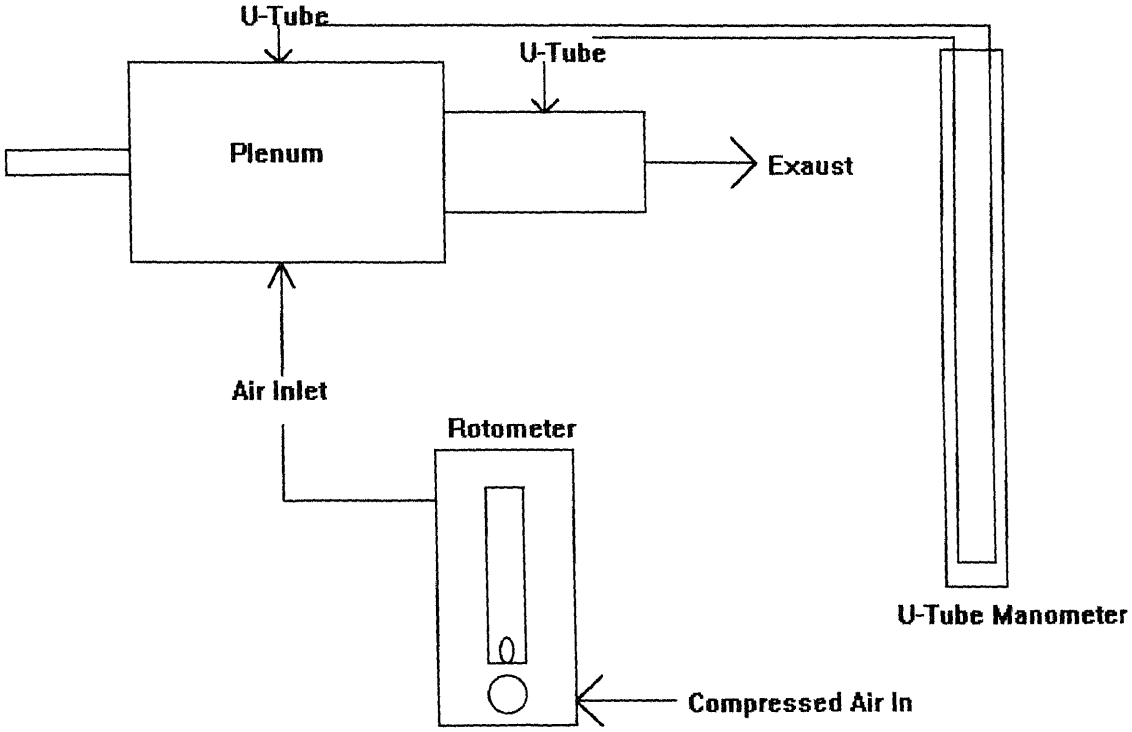

REFERENCES

1. J Kao, R. Pfeffer and G.I. Tardos, "On Partial Fluidization in Rotating Fluidized Bed", *AIChE J.*, vol. 33 (5), pp. 858-861, 1987

2. R. N. Dave, "Experiments and Simulations in Particle Technology" Notes from ME-717-102, NJIT, Spring 1998

3. I.S Fischer, "Introduction to Particle Technology", Notes from ME-717-001, NJIT, Fall 1997

4. K. Leschonski, "Short Course on Selected Topics of Particle Technology", Notes from Short Course, CUTEC-Institute Ltd., Clausthal, Germany, 1998

5. P. Singh and D.D. Joseph, "Dynamics of Fluidized Suspensions of Spheres of Finite Size", *Int. J. Multiphase Flow*, vol. 21, No. 1, pp. 1-26, 1995

6. S. Sasa and H. Hayakawa, "Void-Fraction Dynamics in Fluidization", *Europhys. Lett.*, 17 (8), pp. 685-689, 1992

7. F.A. Zenz and D.F. Othmer, *Fluidization and Fluid-Particle Systems*, Chapman & Hall, London. UK, 1960

8. H. Littman, M.H. Morgan III and C.B. Morgan, "A New Computer Controlled Wurster-type Particle Coating Apparatus", *Advances in Fluidization and Fluid Particle Systems, AIChE Symposium Series* Vol. 93, pp 125-130, 1997

9. M. Rhodes, *Principles of Powder Technology*, John Wiley and Sons, New York, 1990

10. S. Watano, R. Pfeffer, R. Dave and W.C. Dunphy, "Dry Particle Coating by a Newly Developed Rotating Fluidized Bed Coater", *Proceedings from AIChE Convention*, 1998

11. C.Y. Wen, and Y.H. Yu, "A Generalized Method for Predicting the Minimum Fluidization Velocity" *Chem. Eng. Symp. Ser.*, 67, 100, 1966